U.PORTO

FEUP FACULDADE DE ENGENHARIA UNIVERSIDADE DO PORTO

INDOOR THERMAL COMFORT IMPACT OF HEATED AIR INDIRECTLY PRODUCED BY PHOTOVOLTAIC PANELS

ANA CATARINA CRUZ OLIVEIRA

Dissertação submetida para satisfação parcial dos requisitos do grau de

MESTRE EM ENGENHARIA CIVIL — ESPECIALIZAÇÃO EM CONSTRUÇÕES

Orientador: Professora Doutora Ana Sofia Guimarães

Coorientador: Doutor João Quesado Delgado

JUNHO DE 2021

MESTRADO INTEGRADO EM ENGENHARIA CIVIL 2020/2021

DEPARTAMENTO DE ENGENHARIA CIVIL

Tel. +351-22-508 1901

Fax +351-22-508 1446

✉ miec@fe.up.pt

Editado por

FACULDADE DE ENGENHARIA DA UNIVERSIDADE DO PORTO

Rua Dr. Roberto Frias

4200-465 PORTO

Portugal

Tel. +351-22-508 1400

Fax +351-22-508 1440

✉ feup@fe.up.pt

http://www.fe.up.pt

ACKNOWLEDGMENTS

This work is a result of the project "BlueWoodenHouse", with the reference POCI-01-0247-FEDER-047157, co-funded by the European Regional Development Fund (ERDF), through the Operational Programme for Competitiveness and Internationalization (COMPETE 2020), under the PORTUGAL 2020 Partnership Agreement.

Firstly, I want to thank my parents for their unconditional support in every step of my life, for having always helped me in everything I have needed, and for all that cannot be enumerated.

To my brother, although words will never be enough, thank you for always being there for me. Thank you for everything.

To Duarte, thank you for all the support in the most complicated moments and for being the person who most encourages me to be better.

To my friends, thank you for your patience, for all the moments and for making these years of college become the cliché: the best years of my life.

To my thesis supervisor, Professor Ana Sofia Guimarães, and to my co-supervisor, Professor João Delgado, I thank all the patience, understanding, availability, and knowledge transmitted.

To Leonardo, a special thank you for all the support, for the tireless willingness to clarify all my doubts, and for all the follow-up throughout this work. This dissertation certainly would not be the same. A thank you is not enough.

RESUMO

Nesta dissertação é realizado um estudo que pretende analisar a viabilidade de uma solução de painel fotovoltaico que pretende aproveitar o ar quente, indiretamente produzido pelo mesmo, para posterior aquecimento de uma casa. Esta solução consiste numa caixa inserida na parte exterior do painel de forma a armazenar o calor que este produz indiretamente na parte de trás. Esta caixa terá ainda uma conduta responsável por conduzir o ar quente que se encontra dentro da caixa até à casa para que esta possa ser aquecida.

Desta forma, foram realizadas simulações numéricas em estado transiente, com recurso ao software Ansys Fluent, considerando-se para tal um modelo 3D de uma casa com seis painéis fotovoltaicos instalados na cobertura. Dada a complexidade das simulações a desenvolver neste modelo e a falta de informação inicial necessária para que fossem realizadas, efetuar-se-á uma divisão em dois modelos mais simples: um correspondente apenas ao painel com a caixa e um outro correspondente à casa com uma conduta, para a entrada de ar, e uma janela para a saída do mesmo.

As simulações executadas no primeiro modelo tiveram como objetivo a determinação da temperatura do ar no interior da caixa, enquanto as realizadas no segundo visaram concluir que temperatura se poderia atingir dentro da casa com o ar quente proveniente da caixa e analisar a contribuição deste calor para o conforto térmico da casa. Estas simulações permitiram obter a distribuição de temperatura nos dois modelos, tendo sido testadas diferentes condições de forma a ser possível perceber o efeito das mesmas nos resultados obtidos.

Na sequência desta primeira análise, foi feita, posteriormente, uma análise paramétrica em ambos os modelos para um dia típico de Inverno e de Verão às 10:00, 13:00 e 16:00 horas. Tal como nas simulações "teste" realizadas anteriormente, o objetivo é determinar a temperatura dentro da caixa e dentro da casa, mas agora com valores reais. Para a simulação da casa, a temperatura de entrada do ar considerada foi a obtida na simulação do primeiro modelo.

Por fim, com base nos resultados obtidos nas análises paramétricas foi possível concluir que as temperaturas no Inverno não são suficientemente elevadas para que o calor produzido indiretamente pelo painel consiga aquecer uma casa.

PALAVRAS-CHAVE: Painéis fotovoltaicos, Ansys Fluent, conforto térmico, simulações numéricas

ABSTRACT

In this dissertation is carried out a study that aims to analyze the feasibility of a photovoltaic panel solution that intends to take advantage of the hot air, indirectly produced by it, for subsequent heating of a house. This solution consists of a box, inserted on the outside of the panel, that will be used to storage the heat that the panel indirectly produces on the back. This box will also have a duct responsible for driving the hot air inside the box to the house, so that it can be heated.

Thus, numerical simulations were performed, in a transient state, using the Ansys Fluent software, considering a 3D model of a house with six photovoltaic panels installed in the roof. Given the complexity of the simulations to be developed in this model and the lack of initial information necessary for them to be carried out, a division will be made into two simpler models: one corresponding only to the panel with the box and another corresponding to the house with a duct, for the air inlet, and a window as an outlet.

The simulations performed in the first model aimed to determine the air temperature inside the box, while those performed in the second aimed to conclude what temperature could be reached inside the house, with the hot air coming from the box and analyze the contribution of this heat to the thermal comfort of the house. With these simulations the temperature distribution was obtained in both models, different boundary conditions were tested in order to realize their effect in the results obtained.

Following this first analysis, a parametric analysis was subsequently performed in both models for a typical winter and summer day at 10 am, 1 pm and 4 pm. As in the "test" simulations performed previously, the goal is to determine the temperature inside the box and inside the house, but now with real values. For the simulation of the house, the inlet temperature of the air considered was the one obtained in the simulation of the first model.

Finally, based on the results obtained in the parametric analyses, it was possible to conclude that winter temperatures are not high enough for the heat produced indirectly by the panel to heat a house.

KEYWORDS: Photovoltaic panels, thermal comfort, Ansys Fluent, numerical simulations

CONTENTS

LIST OF FIGURES

LIST OF TABLES

1
INTRODUCTION

1.1. FRAMING AND PRESENTATION OF THE WORK

Climate change is one of the most debated issues today around the world, given its global impact.

The construction industry in the European Union (EU) accounts for 40% of energy consumption and 36% of greenhouse gas emissions. Thus, the continuous improvement of energy efficiency in buildings plays a key role in achieving the carbon neutrality goal by 2050.

At a time when the irreversible point of global warming may have already been reached, change becomes urgent, with one of the solutions being the use of renewable energies. Among renewable energies, solar is considered not only one of the most promising ones, but also one of the energies with the greatest potential growth.

Among all low-carbon technology options, accelerated deployment of solar PV alone can lead to significant emission reductions of 4.9 gigatonnes of carbon dioxide. Solar panels have improved substantially in their efficiency and power output over the last few decades and, in addition to the production of electricity, their heat can also be harnessed.

Therefore, the objective of this work is to study a photovoltaic panel solution in which the heat produced indirectly by it will contribute to the heating of a house and, consequently, to thermal comfort.

Through numerical simulations, the flow and temperature distribution will be predicted inside the panel and the house. Different conditions will also be tested on the geometry to see how they influence the temperature results.

1.2. ORGANIZATION OF THE THESIS

This work is divided in five chapters and their subdivisions.

The introductory chapter presents the framework, objectives, and organization of the thesis.

The second chapter, “State-of-Art”, presents a brief summary of the historical evolution of the theme as well as a literature review on what is known about the technologies under study.

The third chapter essentially describes the problem studied, introduces the software used for the numerical simulations and the methodology followed.

The fourth chapter presents the results obtained with the simulations described in the previous chapter and the respective analysis and discussion.

The fifth chapter gives the overall conclusions obtained from this work and future prospects on this topic.

2
CONTEXT AND STATE OF ART

Global energy transformation is inevitable and urgent in order to limitate climate change and promote sustainable growth. Despite rising concern about human-caused climate change, support for the Paris Agreement, and the prevalence of clean and sustainable energy options, energy-related carbon dioxide (CO2) emissions have increased 1.3% annually, on average, over the last five years, which show us that there is, still, much to do and evolve regarding renewable energies [1].

The covid-19 pandemic affected the world in the most diverse sectors, and energy was not the exception. With the lockdown and economic crisis that followed, carbon dioxide (CO2) emissions declined by 7%, in 2020 and investment in clean energy is expected to fall by 8% [2].

According to the World Energy Outlook 2020, renewables meet 80% of global electricity demand growth during the next decade and overtake coal by 2025 as the primary means of producing electricity [2]. By 2030, hydro, wind, solar PV, bioenergy, geothermal, concentrating solar and marine power between them provide nearly 40% of electricity supply [2].

In Portugal, according to the Portuguese Renewable Energy Association (APREN), during 2019, the renewable electricity share represented 52.9% of the national demand, led by the wind technology, with 23 %, followed by hydro technology with a normalized share of 21 %, solar photovoltaics with 2.3 %, bioenergy with 6.0 % and geothermal with 0.4 % [3].

According to the report of RNC 2050, the solar photovoltaic technology will raise up to 13 GW centralized and decentralized in Portugal by 2050 [5].

Solar energy will be one of the dominating sources of energy, and according to Irena, by 2050, 86% of electricity generation would be renewable, with 60% coming from solar and wind [1]. Wind and solar PV would dominate expansion, with installed capacities of over 6 000 GW and 8500 GW, respectively [1]. Based on IRENA's REmap Case, the solar PV share of global power generation would reach 13% by 2030 and 25% by 2050, as shown in figure 1[4].

The levelized cost of electricity (LCOE) for solar PV is already competitive now compared to all generation sources (including fossil fuels) and is expected to decline further in the coming decades, falling within the range of USD 0.02 and 0.08/kWh by 2030 and USD 0.014 0.05/kWh [4].

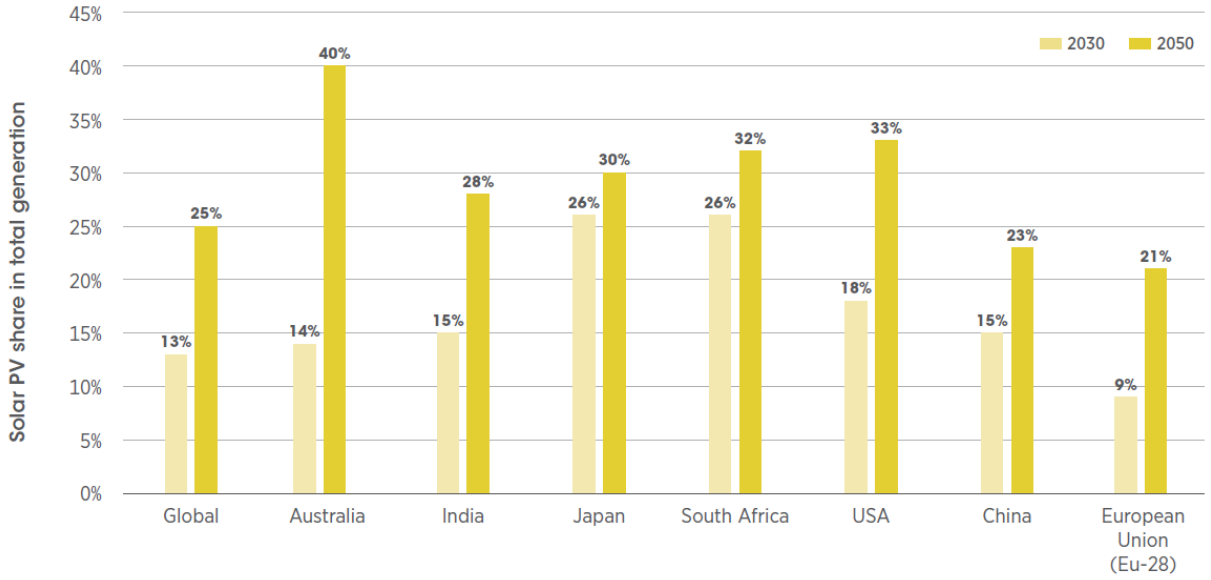

Figure 1: Higher penetration of solar power in electricity grids in various countries by 2030 and 2050 [4]

It is important, in order to increase the utilization of renewable technologies, that a consistency between energy policy and fiscal policy with regards to the fees and taxes applied to renewables as a whole and, particularly, to the electricity generation, exists. There must be created conditions to attract investment and financing.

2.1. BRIEF HISTORY OF SOLAR PHOTOVOLTAICS

In the last decade, there has been a growing concern regarding climate change, which has led to the need to produce and use alternative solutions, being solar energy technologies one of them.

Although solar technologies seem recent, they have been used for more than a century, with scientists working with solar cells for nearly 200 years.

The first huge step in solar panel technology came when Alexandre Becquerel observed the photovoltaic effect in 1839 [6], which consists in the production of electric current when a material is exposed to light due to the potential difference that is generated, but it was only in 1883 with Charles Fritts that the first solar cells emerged. They were made of a thin, wide layer of selenium onto a metal plate and covered it with a semitransparent gold-leaf film to create the first photoelectric module [7].

However, it was only with the great scientific developments in the first half of the 20th century, such as the explanation of the photoelectric effect by Albert Einstein in 1905, the advent of quantum mechanics and, in particular, the theory of bands and the physics of semiconductors, as well as, the purification and doping techniques associated with the development of the silicon transistor, that solar panel technology started to grow and evolve. Without science the “birth” of electric solar power would be unimaginable [8].

On April 25, 1954, Bell Laboratories produced the first modern photovoltaic cell made of silicon, as shown in figure 2, whose efficiency was low:1 watt of electricity costed $250 to produce [6].

Since the efforts to commercialize solar cells were unsuccessful due to their price, the technology started being use for the space program, where it was found to be cost effective [8]. Despite the reluctance to use them, in 1958 Vanguard was the first satellite to use solar cells to back up its main power source,

and while the chemical batteries failed to work after a week, the silicon solar cells continued working for years. Nevertheless, and even though they were not very efficient for terrestrial use, it was the development of solar cells for space utilization that made them more efficient and led to important technological advances in the next decade. One example of this, was the replacement, from 1960, of the single frontal contact by a network of thinner but scattered contacts, reducing serial resistance and increasing efficiency [8].

If during the 1960s and 1970s the development of solar cells was mainly motivated by the space race, making solar panel technology too expensive, but also more efficient, it was in the '60s that the first terrestrial applications emerged. It was the case SOLAREX cells, a company by Joseph Lindmeyer, that started producing photovoltaic panels for remote telecommunications and navigations buoys. These applications turned out to be economically advantageous due to the lack of alternatives sources to solar electricity [8].

The advances of the '60s and '70s drove the price per watt of solar energy from $100 down to around $20, increasing photovoltaic production, which hit 21.3 megawatts in 1983.

The history of photovoltaics enters a new chapter due to the 1973 oil crisis. The panic created led to a sudden investment in research programs to reduce the cost of producing solar cells. New materials, in particular, multicrystalline silicon, instead of the monocrystalline one, started being used as well as new silicon production methods directly on the tape, eliminating the cutting process of silicon ingots and all associated costs. Efficiency wise, the 20% efficiency barrier was reached by monocrystalline silicon cells, in Australia in 1985 [8].

The 1980s and 1990s were marked by the growing concern and awareness of the danger posed by climate change, and the importance of trying to halt its progress, resulting in increased investment in funding programs. Examples of these initiatives are the installation of the first large solar power plant in California in 1982, and the launch of "solar roof" programs in Germany (1990) and Japan (1993). Political forces understood came to the conclusion that the creation of a true photovoltaic market could not be based, solely, on technological development, increasing the efficiency of cells or reducing their cost of production, but also through an economy of scale: The higher the quantity of manufactured cells, the lower is the unit cost [8].

The use of initiatives that stimulate the market has resulted in the growth of the solar electricity market at the end of the nineties and beginning of this century: in 1999 the accumulated total of solar panels reached the bar of the first gigawatt and, three years later, the accumulated total was already double [8].

Solar PV has been one of the pioneering renewable technologies over the decades and is expected to continue driving overall renewables growth in several regions over the next decade.

2.2. PHOTOVOLTAIC PANELS

Amongst the available renewable energy sources, solar energy is not only the most abundant and endless resource, but also the cleanest. To harness solar power, various technologies have been developed, such as: solar lighting technology, solar thermal technology, solar thermal power technology, solar photovoltaic (PV) technology, solar hydrogen production technology, etc. [9]. Solar photovoltaics are considered the most promising one due to their advantages in energy generation, operation and maintenance [10]. Photovoltaic panels are one of the most "popular" devices used to produce electricity from the solar energy.

Solar panels consist of several solar modules, with the latter being made from individual solar cells that are connected to each other [11]. Solar cells are generally composed from layers of silicon doped with boron, in which a positive charge develops, and phosphorous, which generates the negative charge. Solar cells absorb the solar photons which lead to a current being generated through the cells [11]. This process is known as the Photovoltaic or PV effect.

As far as the composition is concerned, various semiconductor materials can be used in PV cells, including silicon-based materials, non-silicon-based materials, and several advanced materials [9]. Silicon is the most used material in commercial solar cells due to its reliability in the solar PV field, representing about 90% of the photovoltaic cell market [12].

Silicon cells can be grouped into three types: monocrystalline (m-Si or mono-Si), polycrystalline (poly-Si or multi-Si) and thin-film amorphous (a-Si). Monocrystalline cells are regarded as the most efficient and expensive cells once the manufacturing techniques used to produce them are rather complex [11]. They are made from a single crystal of silicon which can be sliced and are usually black or gray in color [9]. Polycrystalline PV cells are fabricated from ingots of multi-crystalline silicon with multi-colored shining blue tones. When compared to the monocrystalline ones they are less effective, but also cheaper [9]. In amorphous silicon PV cells, whose color is reddish-brown or black, the PV cells are formed from amorphous materials that are built by spreading a thin homogeneous layer of amorphous silicon onto a surface, creating a thin structure. Hence why they are also known as thin-film cells [11]. In terms of efficiency, for monocrystalline cells, the efficiency ranges between 16% and 24%. The efficiency of polycrystalline cells varies in the range of 14–18% and as for thin film cells the efficiency ranges between from 4% to 10% [9].

Solar PV cells can be divided, again, into three generations of PV technologies. Monocrystalline and polycrystalline are called first generation solar cells, which mean they last longer and have higher efficiency than other cells [9]. However, and even though they are the most widely used cells amongst all the three generations, their cost is higher, and their performance can easily degrade at higher temperature conditions [9]. The second generation consists of amorphous silicon, Copper-Indium-Gallium-Selenium (CIGS), and Cadmium Telluride (CdTe). These cells have a lower efficiency when compared to the first-generation cells and, therefore, cost less. The efficiency of CdTe and CIGS cells varies from 9.4% to 13.8% and from 11% to18.7%, respectively [9].

Third generation PV cells include innovative types of cells whose aim is to make solar PV technology more efficient and less expensive by using a variety of new materials like solar inks, nanotubes, organic dyes, conductive plastics, etc. Since there is, still, a lot of development and research to do regarding this technology, first and second generations PV cells cover the majority of PV markets [9].

Photovoltaic systems can be classified according to the energy supply, the storage modes, the integrating modes, and the modules type [9]. According to the power supply and storage modes, there are two types: the grid-connected type and the stand-alone type. In the first one, the solar system is connected to the utility grid, that acts like a battery with an unlimited storage capacity, and ensure the system's stability, resulting in a better overall efficiency, whereas in the second, systems produce power independently of the utility grid, meaning it will require a battery storage system to storage the excess of energy [13]. Stand-alone systems may also need a supplementary generator for power supply in extreme weather conditions.

A typical photovoltaic solar system, as shown in figure 3, consists of four basic elements: Photovoltaic module, charge controller, the inverter and battery, when necessary, as shown in figure. The inverter is a device that changes the direct power (DC) from the PV array to alternating power (AC) used in the electrical grid or AC loads at home. If the efficiency of the energy conversion of the inverter is too small,

then the power generated by the PV array cannot be output to AC system effectively, compromising the overall performance of the photovoltaic system [14]. As for the charge controller, it has the function to preserve the batteries from being overcharged or discharged completely, increasing its useful life [12]. Lastly, batteries, as said previously, are used in stand-alone systems to store the surplus energy produced by the panels, with the aim of being used at night or on days with less sun [12]. When batteries are used in a PV system, they must be located in an area without extreme temperatures and with adequate ventilation [14].

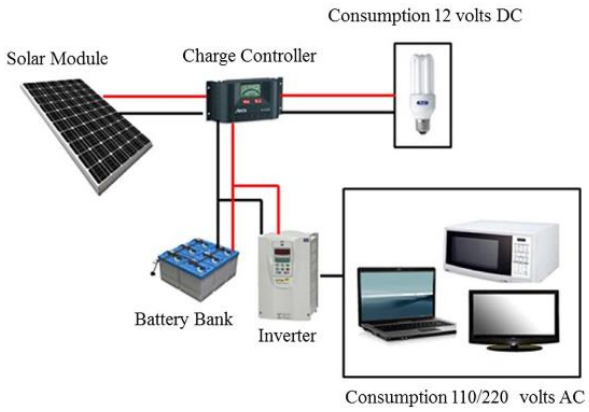

Figure 2: Typical photovoltaic solar system [12]

According to the integration pattern, i.e., depending on the way of installation and construction in the building, the PV systems can be classified as building applied photovoltaics (BAPV) and building integrated photovoltaics (BIPV):

- In BAPV, the PV modules are directly attached to the buildings using additional mounting structure and moving rails. Here, the PV modules do not have any direct effect on the building structures and the way they function. The PV modules are installed at certain tilt angles either on roof or façade (BAPV-wall, BAPV sloped roof) based on local weather conditions. [10]

- In BIPV, the PV modules are integrated within the building structures mainly into roof or façade. Such integrations can also be referred to as BIPV façades and BIPV-roof. Here the PV modules will replace the traditional building materials used for the construction of roof or walls by the BIPV products. The BIPV is installed considering the local weather conditions and the building architecture. [10]

It is important to notice that for having an efficient BAPV or BIPV the factors that influence the performance of both should be considered. These factors include solar radiation, PV technology, PV module temperature, installation angle, tilt angle and orientation, azimuth angle, shading conditions and spectral effects, etc. [10]. The increase of the module's temperature, for example, which happens with the production of energy, will reduce the panel overall efficiency.

Besides roof or façade integration, there are many alternatives for PV integration in buildings, including windows, sunshade integrations, rain-screen integrations, and integration into atrium/skylights, claddings, railings, etc. In the current BIPV market, about 80% of BIPV systems are based on roof integrations, while the rest (20%) are based on façade integrations [9].

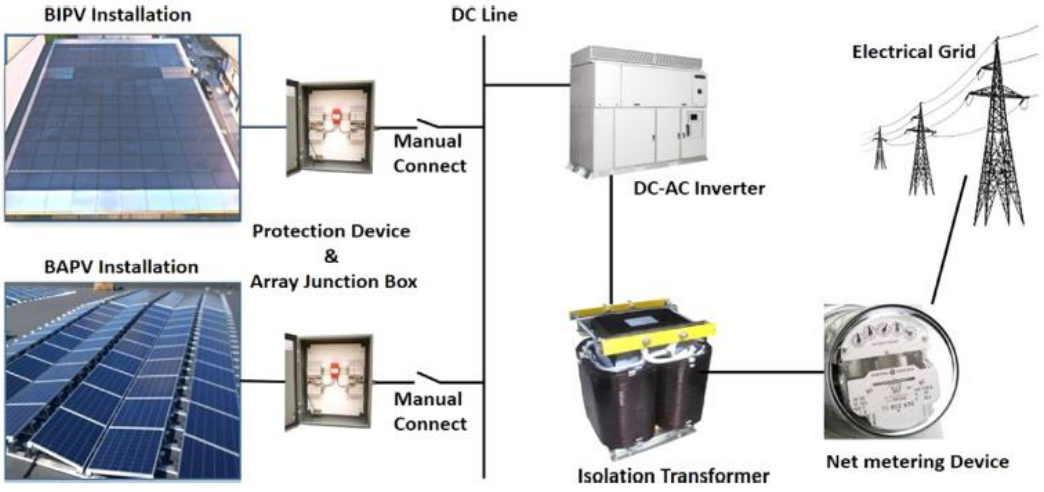

Figure 3: Grid- connected BIPV and BAPV system [10]

According to the module shape, BIPV systems can be categorized as rigid-module-based BIPV systems and flexible-module-based BIPV systems. Rigid BIPV modules can be manufactured from all PV technologies available by employing a rigid back-sheet or rigid substructures such as plastic, glass, or metal sheets. Flexible BIPV modules can be fabricated from most emerging technologies like perovskite-PV technology, dye-sensitized PV technology, organic PV technology, and all thin-film technologies, including CIGS, CdTe, amorphous silicon, etc. The substructure of flexible PV modules can be polymer films or metal sheetings [9].

BIPV systems can be classified as opaque systems and semi-transparent systems. In opaque systems no sunlight is allowed to pass through the system into the indoor environment, while semi-transparent BIPV systems can be built in see-through building envelope components, such as façades, windows, atriums, skylights, etc. In semi-transparent BIPV systems, conventional glazing materials are replaced by semi-transparent PV modules [9].

2.2.1 ADVANTAGES AND BUILDING INTEGRATION OF BIPV

BIPV, as previously mentioned, refers to the integration of PV materials into building envelopes by replacing traditional building materials and producing electricity on-site. Integration improves cost effectiveness by having the PV panels provide additional functions that involve active solar heating and daylighting. BIPV has significant advantages over the more usual "add-on" strategy [15]. Additionally, not only does it eliminate an extra component (e.g., shingles) but it also eliminates penetrations of a pre-existing envelope that are required in order to attach the panel to the building [15].

Integrating PV elements into buildings helps them to achieve self-sufficiency in terms of electricity. The electricity produced can be partially or fully used to meet the energy needs of the house, thereby mitigating the power supply pressures of traditional electricity grids and further reducing fossil fuel consumption and greenhouse gas emissions. In fact, BIPVs shows a high level of innovation and the potential to build green or zero-energy buildings in the future [9].

Besides the electricity production there are other advantages associated with BIPV. For instance, in summer, adding PV modules to building envelopes can help to reduce the heat gain, once they are not being directly exposed to solar radiation, thus effectively reducing the indoor cooling load. Reserving an air channel between the PV modules and the external envelopes of a building may be beneficial to

the system, since the air circulation in the channel leads to a decrease of the PV modules temperatures, increasing, this way, the energy efficiency of the PV panels [9].

In addition to the advantages of BIPV, another important aspect to be taken into account is their suitable integration in buildings. PV modules are designed for electricity generation, which means that their functionality as an envelope element is often overlooked by PV module manufacturers. Being able to make all these technologies suitable for being incorporated in building envelopes while guarantying some essential requirements of PV modules, like considering their properties of being mechanically stable, fire resistant, providing sound and thermal insulation, etc., is a challenge for architecture [9].

There are several options for the integration of PV modules into buildings, including roofs, walls, windows, and shadings. Furthermore, some modules can be flexible, decorative, and visually arresting, allowing architects and designers to produce a variety of visual effects while still making buildings environmentally friendly [9].

PV module technologies, such as PV modules, PV laminates, and PV tiles are now available in the PV industry. PV laminates were developed by removing the frame of PV modules, while PV tiles were created specifically for roof applications. All of these PV modules can be made of opaque or semitransparent materials. The light transmission of PV modules or PV laminates made from mono- or poly-crystalline silicon technologies can be regulated by adjusting the cell spacing [9].

Moreover, the applicability of existing PV modules shows that there are several options that can be used depending on integration, i.e., whether it is sloping roofs, flat roofs, walls, windows and shading systems. For example, standard PV modules with a rigid frame and a non-transparent back-sheet are well suited for use on sloped roofs, but are inadequate for use on flat roofs, walls, floors, or shading systems, while PV laminated modules, on the other hand, can be used on everything except for windows [9].

In general, integrating PV technology into buildings not only allow us to produce electricity on-site, but it also provides some additional benefits in terms of architectural aesthetics and energy efficiency. When compared to traditional buildings, these PV integrated buildings have better natural lighting, enhanced thermal comfort, and lower energy consumption [9].

2.2.2 PERFORMANCE OF BIPV PANELS

The main aspects to be considered regarding the performance of BIPV panels are the electrical and thermal efficiency.

The conversion efficiency of a photovoltaic panel corresponds to the percentage of power collected and converted into electricity [14]. The higher the conversion efficiency, the higher the electricity generation is, and this will depend on the PV module employed.

Several types of PV technology can be used in PV modules and National Renewable Energy Laboratory of the U.S reported the efficiencies of various PV technologies from laboratories, universities, and companies, including multifunction PVs, crystalline silicon, thin-film, and other emerging PV technologies, as shown in figure 4 [16].

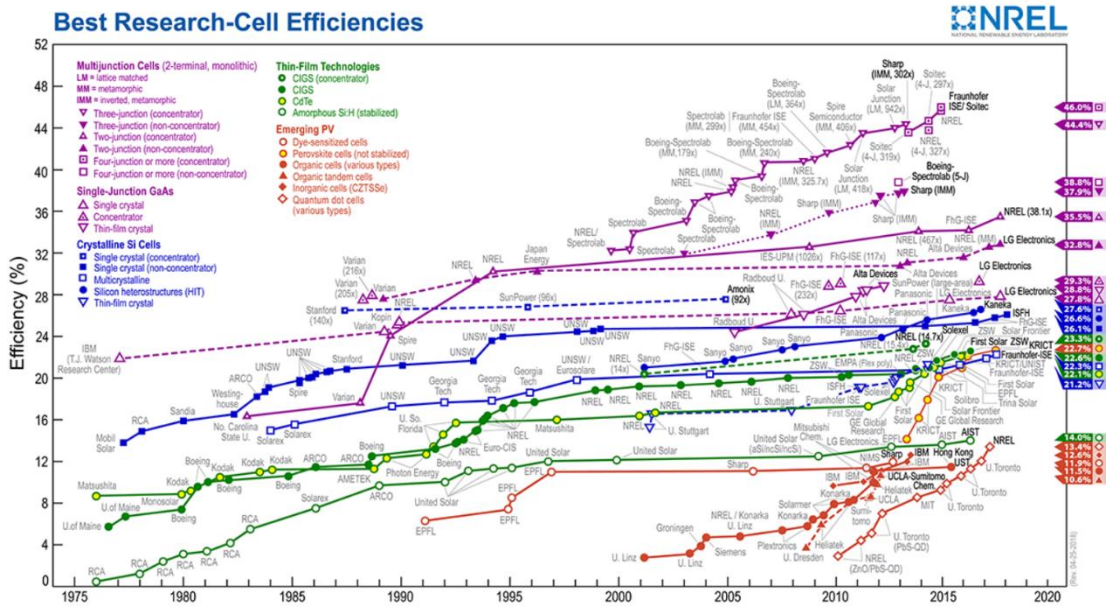

Figure 4: Solar cells energy conversion efficiencies [9]

Besides module efficiency, other parameters can influence the performance of a BIPV system, such as solar irradiance, system orientation, temperature of the module, incident and azimuth angles, shading effect, etc. [9].

The quantity of power coming from solar source per unit area is known as irradiance. Irradiance usually fluctuates according to the weather and the sun's location in the sky. Solar irradiation impinging on a surface consists of direct, diffused, and reflected radiations. The largest fraction of the solar irradiation is the direct component; however, all diffuse and reflected radiation must be considered during the analysis of the system [14].

As the solar irradiance increases, the electrical power output from the PV panel increases too. The relationship between the module current and the solar irradiance is approximately linear [14].

A research about the electricity generation of a thin-film BIPV system under different solar incidence angles and various azimuths shows that when the system was facing south with a slope of 30°, produced the maximum amount of electricity, which did not occur when trying other angles [9].

Another critical factor affecting the power output of BIPV systems is the operating temperature. Just 1 °C rise in a c-Si PV module's working temperature is enough for the power to decrease 0.52 percent and 0.48 percent in standard outdoor conditions and normal test conditions, respectively. In an attempt to find a solution for the temperature modules, a simulation to study the effect of adding a backside air gap on, was performed. The results indicated that a 12–16 cm air gap could greatly reduce the overheating problem and increase the electricity generation [9].

As mentioned above, thermal efficiency is another important aspect when it comes to the performance of a BIPV system. The shading effect of PV modules in BIPV systems will substantially reduce heat gain through external envelopes, impacting the heating or cooling load and further reducing the energy requirements of indoor systems [9]. In addition, the output power from PV panels will be lowered due to the shadowing effect. Shadows can be caused by poles, trees and buildings and may also be caused by the module mounting structures on other structures, preventing solar radiation from reaching the panel [14].

Studies carried out in four rooftop PV systems revealed that the ventilated PV roof enjoyed a higher power efficiency and lower cooling load, making it more appropriate for summer applications [9].

As in the production of electricity, also thermal performance can improve with the existence of an internal air gap in a glazed PV structure, since the movement of the air takes away the accumulated heat [9].

2.3 LIFE CYCLE ASSESSMENT OF PV SYSTEMS

PV technology can be considered almost completely clean, however, when considering the whole life cycle of the PV system, from silica extraction to system installation, the energy consumption and emissions to environment cannot be ignored.

In order to investigate the environmental performance of PV systems, a life cycle assessment (LCA) is usually conducted to evaluate their environmental impacts during their life cycle. LCA takes into account all the activities involved in the creation of a product, such as the material extraction, manufacturing, transportation and distribution, use and disposal [17].

The International Energy Agency reported the guidelines for a PV system LCA recommended by the International Organization of Standardization. These guidelines could be summarized as three main steps: identifying the technical specifications and characteristics of PV systems; specifying the modeling approaches of an LCA of PV system and reporting and sharing the LCA results of PV system [9].

The energy payback time (EPBT) and the greenhouse-gas emissions (GHGEs) are the most frequently used indicators for the LCA of PV systems. EPBT is defined as the period required for a renewable energy system to generate the same amount of energy that was used to produce the system itself [18]. GHGEs are estimated as an equivalent of CO_2, so we can say GHGEs is the equivalent to CO_2 emission rate, that is a useful index to know how much the PV system can mitigate global warming [18]. These indices can be calculated by the following equations [20]:

$$\mathrm{EPBT(year)} = \frac{\text{Totally primary energy required throughout its life cycle (J)}}{\text{Annual power generation (J/year)}} \quad [1]$$

$$\mathrm{CO_2\ emissions\ rate(g-CO_2/kWh)} = \frac{\text{Totally } CO_2 \text{ emission on life cycle (g-C)}}{\text{Annual power generation(kWh/year)} \times \text{lifetime (year)}} \quad [2]$$

The results of an investigation of a rooftop BIPV system (grid-connected) in Hong Kong, reported by Lu and Yang, revealed that the EPBT of the system was 7.3 years, and the greenhouse-gas payback time (GPBT) was estimated to be 5.2 years by considering the fuel mixture composition of local power stations. This study also showed that depending on the different orientations of the BIPV/T, the energy payback would be different too, ranging from 7.3 to 20 years [19]. It is important to note that lifetime of PV panels is about twenty to twenty-five years, sometimes more.

In a similar way, an energy analysis, environmental LCA, and economic analysis was performed to study the performance of a domestic BIPV system. The energy analysis determined that the system paid back its energy in just 4.5 years, while the environmental LCA revealed that throughout the life of BIPV system, the impacts of production were offset by the electricity generated to provide a net environmental benefit [9].

Different PV systems have different EPBT and GHG emission rates, therefore a study, conducted by Peng et al., was made involving five PV technologies with different materials, in order to compare the energy benefits and environmental impact of the panels [21]. The materials compared were mono-crystalline (mono-Si), multi-crystalline (multi-Si), amorphous silicon (a-Si), CdTe thin-film (CdTe) and CIS thin-film (CIS) and the results are represented in figures 5 and 6:

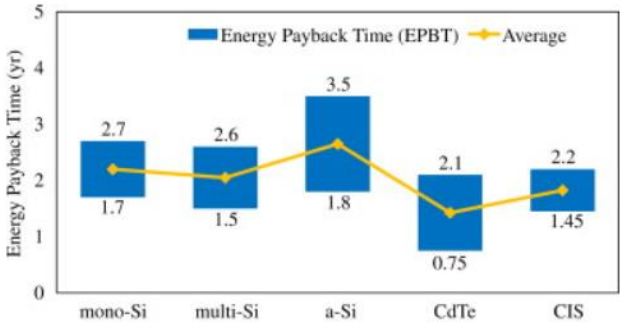

Figure 6: Energy payback time for various PV systems [21]

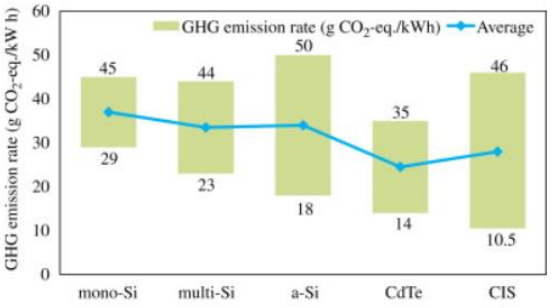

Figure 5: GHG emission rate for various PV systems [21]

From these two figures, CdTe PV system has the shortest EPBT and the least GHG emission rate, rate due to its low life-cycle energy requirements while the mono-Si and a-Si PV systems have the worst performance due to their large energy requirements in life cycle and low energy conversion efficiency, respectively [21].

Both EPBT and GHGE rate of a PV system are influenced by various factors including the solar radiation level, installation location, climate conditions, and other parameters that affect the system's electricity output. Therefore, contrasts between the different types of PV systems will exist. For example, even though the mono-Si PV in figure 2.10. has a payback time that ranges from 1.7 to 2.7 years, if the location were other, these values would be potentially different [9].

Nevertheless, generally, mono-Si PVs have the highest EPBT, while thin-film PVs have the lowest EPBT value. It is expected that new emerging technologies will allow the development of PV materials with higher performance and lower cost leading to PV systems with lower EPBT and GHGE prices [9].

2.4 PV/T SYSTEMS

About 6 to 18% of the incident solar energy is converted to electrical energy by PV panels, with the remaining energy to be heat lost to the outdoor environment [15].

As mentioned previously, PV panels, by producing electricity, also increase the temperature of their cells which results in a reduction of the cells efficiency. The PV/T panel is presented as a solution to this problem, once, while the PV cells generate electricity, the solar thermal absorber collects the heat from the cells, reducing their temperature and improving the system efficiency. A combination between solar thermal collectors and PV panels can be made to form a single module called photovoltaic/thermal system (PV/T), which is a hybrid technology consisting of solar photovoltaic cells and solar thermal components into a single module to generate both electricity and heat in order to improve the efficiency of solar conversion [22].

Through PV/T systems, both hot water and electricity demand for a household can be supplied through a clean renewable energy source [11]. With electricity being the main priority, it is necessary to operate

the PV modules at low temperature in order to keep the PV cell electrical efficiency at a sufficient level [23]. For this reason, the heat produced is mainly of a low temperature and can be used only for low-temperature heat demand, such as domestic hot water production, for example.

As with photovoltaic systems, PV/T systems can also be integrated, with these being called building-integrated photovoltaic/thermal systems (BIPV/T).

According to the International Energy Agency, buildings account for 32% of the world's energy consumption. By generating both electrical and thermal energy, BIPV/T offers an effective way to reduce building energy consumption and, consequently, influences building energy performance owing to the following factors [24]:

- Part of the incident solar energy is directly converted into electricity by the PV module before transmitting through the envelope.
- Part of the absorbed solar energy is removed in the form of heat when a cooling medium is used.
- A BIPV/T component changes the U-value of the building envelope, thus the heat flow between the ambient and the indoor environment is adjusted.
- A PV module obstructs the solar radiation on the original wall.
- The solar absorptivity of a building envelope is changed when conventional building structures are replaced with PV modules.
- The use of semi-transparent PV modules changes the visible transmittance of light and subsequently the artificial lighting energy consumption profile.

Solar radiation is received by the BIPV/T system through a flat surface or a refractive/reflective concentrating device. Amongst the media used to cool the PV are air, water, and refrigerants [24]. A BIPV/T system can be categorized as shown in figure 7:

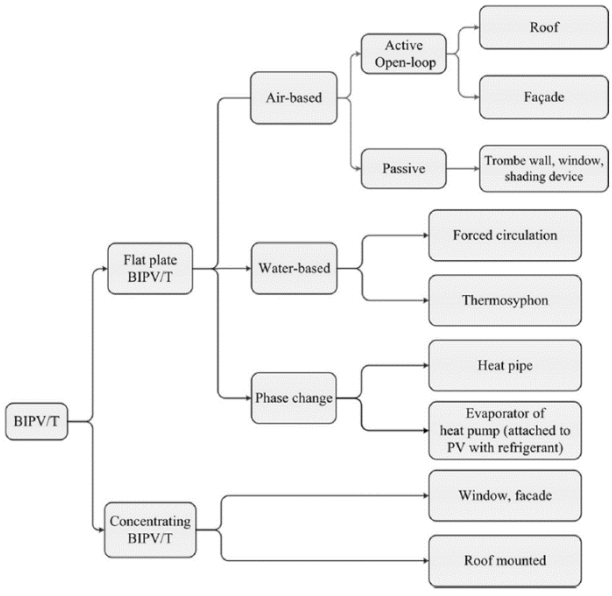

Figure 7: Categorization of BIPV [24]

2.4.1 AIR BASED BIPV/T SYSTEMS

In air based BIPV/T systems, air acts as a working fluid and it is used to keep the temperature of the panel at optimum levels [22]. Additionally, besides the electricity generation, the system can be used for ventilation and heating needs. BIPV/T's use a flat plate air collector that absorbs and collects energy from the sun [22]. Figure 8 presents the basic air-based PV/T and BIPV/T design with the PV/absorber on the outer layer, an air channel for air circulation and an insulated back surface.:

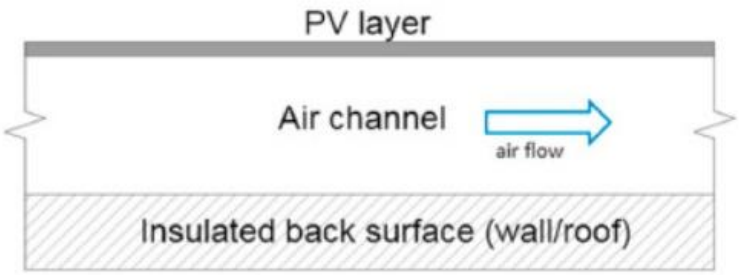

Figure 8: Basic air-based PV/T design

The heat stored in PV's is dissipated through radiative exchange with the sky, convection with the outdoor air and exchange with solid surfaces surrounding the BIPV/T channel [24]. Depending on the applications, BIPV/T panels can be encapsulated, glazed, or insulated. A typical BIPV/T air system is shown in figure 9 [11].

The addition of a cover glass in PV panels increases the thermal efficiency of the system, while the electrical one is reduced due to diminished solar input through the glazing, additional absorption and higher PV temperature [24]. Integrating fins to the back of the PV is another solution that results in a similar increase in thermal efficiency, but that, unlike the glazed solution, does not compromise the electrical output [24].

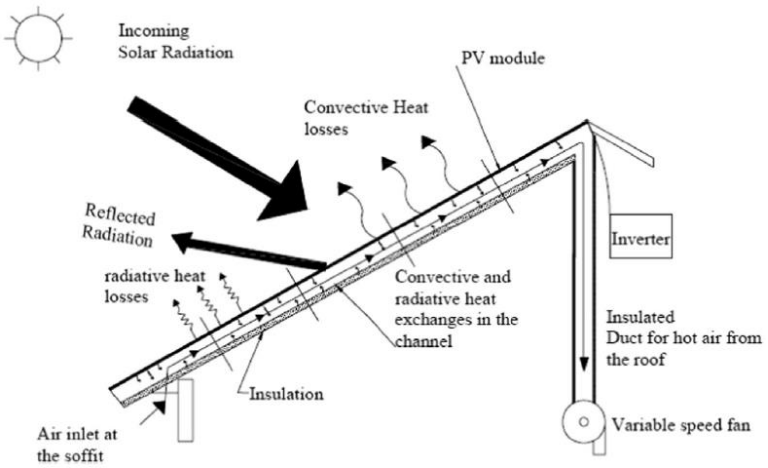

Figure 9: Typical BIPV/T AIR System [24]

Integrating the BIPV/T with an existing building energy system, such as the unglazed transpired collector (UTC), may be beneficial. A UTC is a perforated, dark-colored, and corrugated metal panel that is typically installed on a building's equator-facing façade and has a thermal efficiency of 65-75 %.

With all sides sealed, the ambient air is drawn through the holes and heated along its flow path by the absorbed solar energy. This is, however, more useful to enhance thermal efficiency [24].

It is important to note that simulations were made that showed that not all zones in BIPV/T systems are heated, and thermal efficiency will depend on which zone the heated air is directed to. Air mass flow rate is another aspect to consider when evaluating the efficiency of a system, since an experiment was conducted to evaluate the effects of it on the efficiency of the system, and it showed that the increment in the mass flow rate will increase the electrical efficiency, due to reduction in the system losses [22].

2.4.2 WATER BASED BIPV/T SYSTEMS

BIPV/T water collectors, on the other hand, use a water as a heat removal fluid. This collector turns out to be more effective than air type, because of the temperature variation in liquid is much lower compared to the air, that is based on fluctuation of solar intensity levels [22]. The thermal performance of water collector is affected by the absorptivity of solar cells, but also by the absorptivity of the module area not covered with cells, by transmission losses through the upper glazing and by the thermal conductivity between the PV and the thermal absorber [24].

Figure 10 shows examples of thermal absorbers used in BIPV/T water systems:

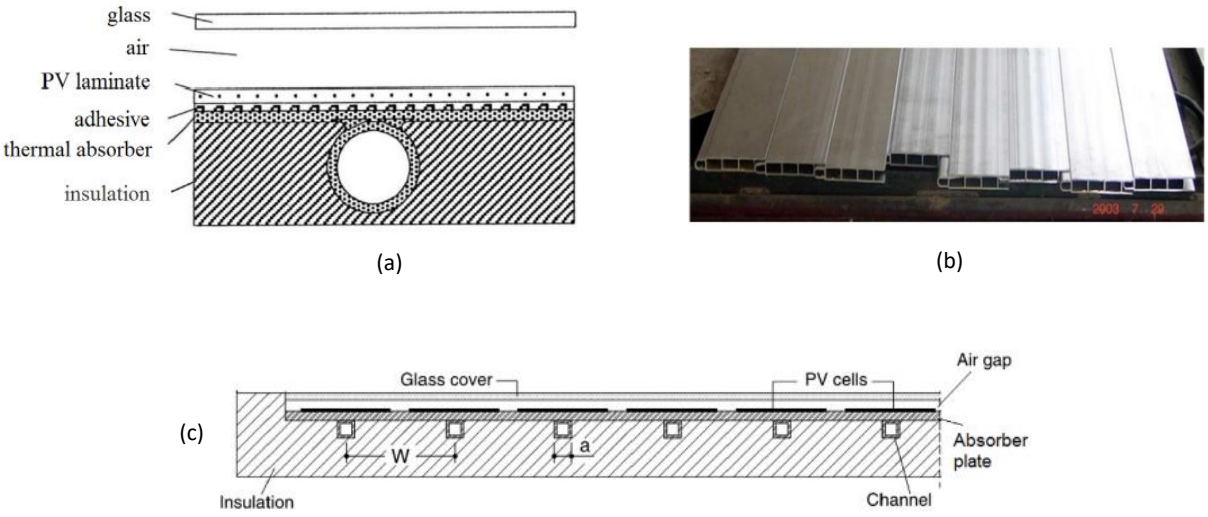

Figure 10: Thermal absorbers used in BIPV/T water systems; (a) Sheet and tube configuration; (b) Flat-box absorber; (c) Rectangular water channels [24]

The sheet and tube PV/T configuration can achieve satisfactory efficiencies, while still being easy to fabricate. The flat-box absorber and rectangular channels, figures (b) and (c), respectively, are used to enhance heat transfer in the BIPV/T system [24].

For instance, a BIPV/T water system with a thermal absorber using rectangular stainless-steel tubes has a combined thermal and electrical efficiency between 55-62% [24].

Furthermore, a laminated BIPV/T collector can achieve higher electricity and energy outputs than side-by-side PV and thermal collector installations covering the same area [24]. Additionally, to increase the

thermal interaction between PV and the thermal absorber, a PV module with a metallic substrate can be used. A PV/T prototype using this type of PV module showed a 10% increase of power generation [24].

Polyethylene pipes can be considered as a thermal absorber by adhering them to the back surface of PV modules [24]. An experimentally tested thermal model revealed that this BIPV/T system outperformed the bare PV system in terms of overall energy efficiency. Polyethylene pipes represent a good cooling solution for PV systems, once they, not only, are economical and require easy maintenance, but also do not disturb the original PV system structure [24]. A BIPV/T system with polyethylene tubes can be installed as the roofing panel onto traditional roof framing and provide thermal insulation.

AS Kalogirou studied water PV/T solar systems for domestic hot water applications. Two types of PV/T systems were considered: a domestic thermosyphonic system and a large size system with PV/T modules placed on a horizontal building roof with the water storage tank located inside the building and a pump for the water circulation [23].

Thermosyphon systems use natural convection to heat and transport the heat transfer fluid from the collector to the reservoir. As thermal fluid is heated up in the collector, it becomes less dense and rises into the top of storage tank [23]. There it is replaced by the cooler water which flows down the collector. This circulation is continuous and lasts as long as there is sun [23].

In direct circulation systems, a pump is used to force the circulation of the water from the collector to the reservoir, with the temperature of the fluid in the collector being higher than the stored water. As a pump circulates the water, the collectors can be mounted either above or below the storage tank [25].

The results showed that PV/T systems achieved an increase of the total energy output, when compared to a standard PV system, since in the latter the heat is lost to the ambient. On the other hand, the electrical output is higher in standard PV modules, once they can operate at higher temperatures [23].

Besides air and water-based systems, there are also BIPV/T systems involving phase change processes. When undergoing the phase change process, materials have a high thermal capability. PV modules temperatures can be held at lower temperatures by adding a solid-liquid phase change material (PCM) cavity at the back of the PV module [24]. Heat pipes with a liquid-vapor phase change process can be integrated in a BIPV/T system [24].

Heat pipes have high thermal conductivity, which may enhance thermal performance and help achieving more uniform PV modules temperature [24]. Figure 11 shows a typical heat pipe system:

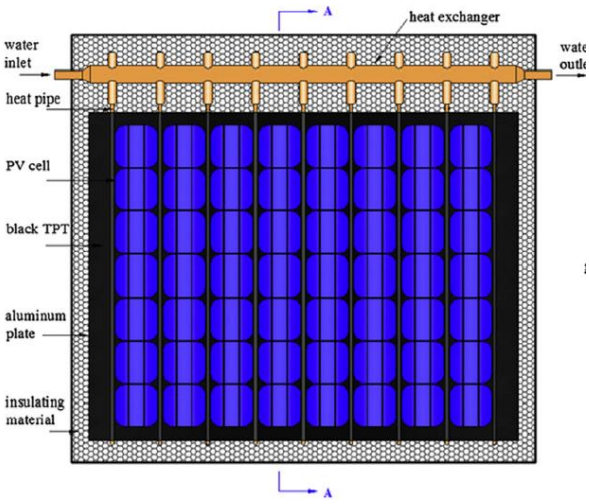

Figure 11: Typical heat pipe system [24]

The heat pipe evaporator attached to the PV module's back collects and transfer the heat to the medium. The vaporized medium then travels to the condenser division, where it releases heat and transitions to a liquid state. The liquid returns to the evaporator via capillary force through a wick structure and another heat transfer cycle begins [24].

The thermal and electrical efficiencies of a heat pipe PV/T system are of 41.9% and 9.4%, respectively [24]. These values can be improved by optimizing the refrigerant and enhancing the heat exchange between the heat pipe and water tank [24].

Even though integrated PV/T panels have several advantages, it has been noted that the market for this technology is still limited [11]. The cost of a PV/T system can be almost twice as much as a typical PV or thermal solar system, with a payback period of up to twenty years. Currently, this period can also be lower due to the newer optimized PV/T systems [11].

The disadvantages of this technology are related to thermal limitations, since the heat produced is mainly of low temperature because of the panel, but also with the need for a complex system design which can comprise several additional components that are required to operate the system efficiently [11]. These components, for example, include thermal storage tanks, controllers, pumps, regulator, inverter, and batteries. This might, therefore, result in a higher system cost and as a result, a longer period of return when compared to other solar technologies [11].

2.4.3 BUILDING INTEGRATION OF BIPV/T SYSTEMS

Nowadays, it is possible to have aesthetically pleasing buildings using photovoltaic panels. Photovoltaic panels integrated into buildings should satisfy the following criteria, according to the report of IEA-PVPS (International Energy Agency Photovoltaic Power System Programme) [24]:

- Natural integration that is architecturally pleasing.
- Good composition between materials, colours and dimensions.
- Consistency with the building concept and framework.
- Well-engineered and innovative integration.

Currently, as referred in 2.2.1, the solar manufacturing industry is developing new materials and technological solutions, so that photovoltaic panels do not constitute an obstacle to architecture. A BIPV/T system should blend in with the building effortlessly to achieve an integral appearance.

An example of the integration of a BIPV/T system is The John Molson School of Business (JMSB) building at Concordia University, Canada, where a BIPV/T air system is installed in the façade, as shown in figure 12. To achieve a pleasing visual effect, the PV modules were custom designed to match the dimensions of the curtain wall structure that covers the rest of the façade [24].

Figure 12: BIPV/T System of the JMSB Building [24]

The aluminum frames and the backsheets of the PV modules are black to allow a homogenous appearance of the BIPV/T system consisting of PV modules mounted onto the black transpired collector, but also to increase solar absorption and thermal efficiency of the BIPV/T system [24]. Later, PV modules were also integrated into the roof, providing a protective layer to the original roofing material without adding a significant visual obstruction to the original roof [24].

BIPV/T systems have a dual function: Produce energy and simultaneously replace the traditional building envelope. As such, it is important to consider some factors such as orientation, building's use and electrical loads, location, climate, snow, and wind loading conditions, etc. while taking into account the design of the building and its materials in order to minimize visual impact [26].

For example, it was stated that the metal roofing underneath the PV modules could cause noise due to windy weather in an energy solar house that was built with a fully roof integrated BIPV/T air system [24]. This demonstrates the necessity of proper structural engineering in the design of BIPV/T systems as a functional building envelope. It is therefore essential to develop standards and codes for BIPV (BIPV/T) technology that impose safety and performance requirements [24].

2.4.4 Concentrating BIPV Systems

BIPV concentrating systems work by concentrating the solar flux or thermal energy onto a small area [11]. A high density of luminous flux is cast on a relatively small PV surface with the use of reflective/refractive devices, resulting in a significantly high solar cell temperature. A thermal collector may be added to reduce cell temperatures while producing high-temperature fluid that can be used for solar heating or cooling [24].

One of the obstacles to the growth of the BIPV systems is not only the price of the electricity, that should be lower in order for more people to use it, but also the cost of the system itself. Concentration technology can reduce the cost of BIPV by reducing the silicon surface without compromising its performance [24]. Concentrator-photovoltaic systems (CPV) use cheap optical elements such as Fresnel lenses or mirrors with minimal reflection. The concentrator increases the luminous flux on PV surface, so fewer PV materials are needed.

Regarding the thermal part the concentrating technology can also have advantages. Contrary to what happens in BIPV/T, in which the thermal system can only provide the produced heat at low temperatures due to the low temperature at which the panels have to operate, the concentrating systems can provide heat at higher temperatures.

Davidsson et al. developed a multifunctional PV/T window, as shown in figure 13, that is integrated into the building [27]. Photovoltaic cells were placed on absorbers, which were positioned in the window behind glazing, in order to reduce construction costs by saving the frames and glazing, and tiltable reflectors were designed in such a way to focus solar radiation on solar cells to improve PV performance. Reflectors provide the ability to control the radiation that is transmitted to the building: If the reflectors are tilted into the vertical direction, the sunlight focuses on the absorber, if the reflectors are inclined in a horizontal direction, sunlight can enter into the building for passive heating [27].

A simulation model for electricity and hot water production was made and results showed that in comparison to the vertical flat PV, the proposed window produces annually about 35% more electricity per unit area of the cell [27].

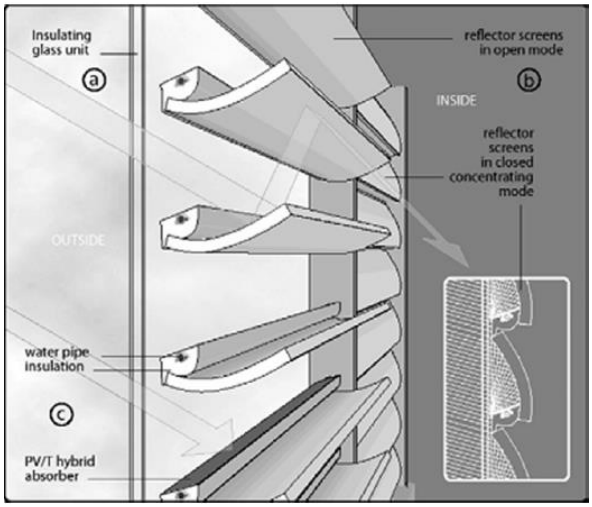

Figure 13: Window-integrated concentrating BIPV/T system [27]

Besides electricity generation, the heat from photovoltaic panels can also be harnessed without them being associated with thermal collectors.

The solar building, in Lisbon, has a photovoltaic system integrated in the façade, which aims to recover the heat produced in the panels and use it to heat the indoor air. In this case, it is natural convection heating: the indoor air of the room heats up when circulating in contact with the interior surface of the panels, re-entering heated into the room. In the next chapters a solution of harnessing heat from photovoltaic panels, installed in the roof of a house, with the purpose of heating the indoor air will be discussed.

3

NUMERICAL SIMULATION METHODOLOGY

3.1. PROBLEM DESCRIPTION

The main objective of this work is to analyze a photovoltaic panel solution installed on the roof of a house, whose heat, produced indirectly in the back of the panel, will be recovered in order to heat the indoor air. The solution under study consists of a box, inserted outside the panel where the heat will be stored, and a duct, introduced in the same box that will be responsible for conducting the heated air to the house interior.

In this chapter, the methodology developed to analyze the thermal comfort provided by six panels installed on a roof will be discussed.

To do so, this case will be divided in steps, each step corresponding to a different model subject to several numerical simulations using the ANSYS® Fluent software.

Ansys Fluent is a fluid simulation software known for its advanced physics modeling capabilities, needed to model flow, turbulence, heat transfer, reactions for industrial applications ranging from air flow over an aircraft wing to combustion in a furnace, among others. For flows involving heat transfer Ansys Fluent solves the continuity, energy, and transport equations. For this work, given that the heating of the air and its subsequent insufflation into the house are being analyzed, Ansys Fluent will be used to study the air flow and the heat transfer that occurs in the models. Essentially, it is fluid mechanics applied to a building.

3.1.1. MODEL'S GEOMETRY

As aforementioned, in this work will be considered a simplified house with six panels installed on the roof. A model of the house and its dimensions are shown in figure 14, where L stands for length, W for width, H for height and T for thickness. ANSYS® SpaceClaim was used to build all the 3D geometries.

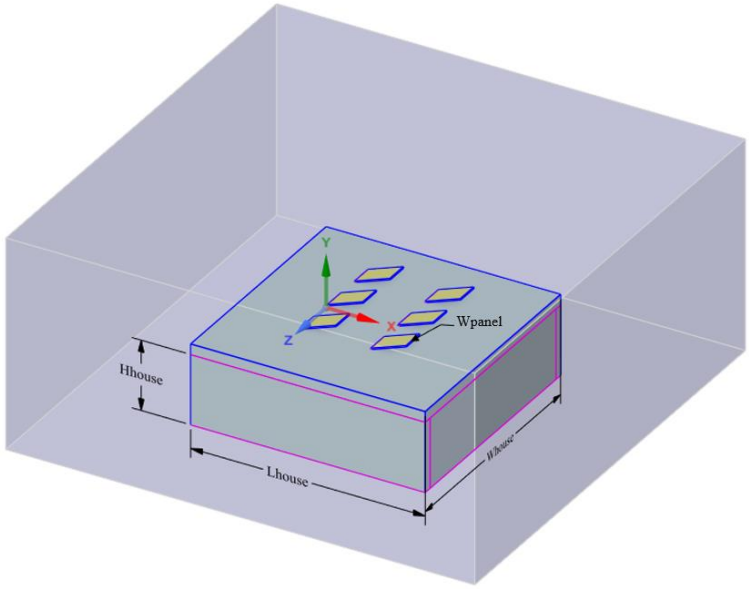

a)

DIMENSIONS/m	
L_{HOUSE}	10
W_{HOUSE}	10
H_{HOUSE}	3
T_{WALL}	0.3
L_{PANEL}	1.6
W_{PANEL}	1
T_{PANEL}	0.05
α_{PANEL}	20º

b)

Figure 14: a) House model; b) House dimensions

In this model, the enclosure represents the fluid domain (air) while both, the house and the panels, represent the solid domain. The enclosure was used to define the control volume where the air flow outside would also be simulated.

Since it would be very complicated to start the simulations in a macro scenario, like the one in figure 14, given the complexity of the model and lack of initial information, the study of this case will be divided into two models: one corresponding only to panel and another one corresponding to the house.

The first model, shown in figure 15, corresponds to one photovoltaic panel, with the same dimensions as each in figure 14, alongside with the box, whose walls are 10 cm thick. The air inside the box constitutes the fluid domain, while the box (in yellow), the PV panel (in green) and the roof (in orange) represent the solid domain. The simulations in this model aim to understand how heated the air inside the box can be when subjected to solar radiation. Basically, this model represents the heat coming from the photovoltaic panel that is intended to be stored for later use in the heating of the house. The purpose of these simulations is to determine the temperature of this stored heat.

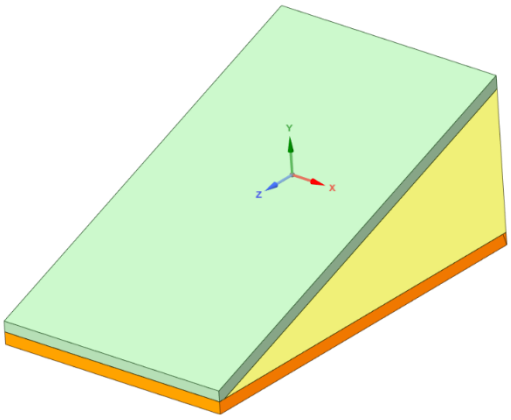

Figure 15: Photovoltaic model

The second model, shown in figure 16, consists of a house, with the same dimensions as the first one, with a duct air inlet and a window as an outlet. The inlet's 10 cm diameter was an assumed parameter. Since the air flow is being analyzed, besides an inlet, an outlet is needed. In this case, it is intended that the outlet is realistic, but at the same time not too small due to the exit velocities of the air, thus opting for a window.

In this model, the temperature determined in the previous step will be used as the initial temperature at which the air enters the house, i.e., the inlet temperature. The aim of the simulations in this model is to understand the contribution of the photovoltaic panel's outside indirectly heated air to the indoor air temperature, whether or not it will contribute to the thermal comfort of the house.

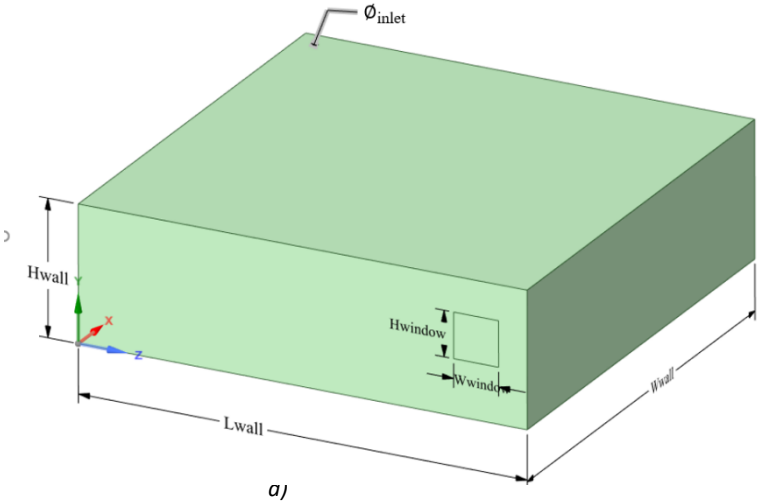

a)

DIMENSIONS/m	
L_{WALL}	10
W_{WALL}	10
H_{WALL}	3
T_{WALL}	0.3
H_{WINDOW}	1
W_{WINDOW}	1
$Ø_{INLET}$	0.10

b)

Figure 16: a) House with a window model; b) House dimensions

3.2. VISCOUS AND RADIATION MODEL

The temperature distribution in these models was obtained in transient state, using the CFD package ANSYS® Fluent.

Among the many options available, standard k-epsilon enhanced wall treatment was the viscous model used in all simulations. The standard k-epsilon model, proposed by Launder and Spalding, is a semi-empirical model, whose robustness, economy, and reasonable accuracy for a wide range of turbulent flows explain its popularity in heat transfer simulations [28]. It was mainly used in these simulations due to its good convergence.

Standard k-epsilon is a two-equation model based on model transport equations for the turbulence kinetic energy (k) and its dissipation rate (ε) [28]. The turbulence kinetic energy, k, and its rate of dissipation, ε, are obtained from the following transport equations:

$$\frac{\partial}{\partial t}(\rho k)+\frac{\partial}{\partial x_i}(\rho k u_i)=\frac{\partial}{\partial x_j}\left[\left(\mu+\frac{\mu_t}{\sigma_k}\right)\frac{\partial k}{\partial x_j}\right]+G_k+G_b-\rho\varepsilon-Y_M+S_k \quad [3]$$

$$\frac{\partial}{\partial t}(\rho \varepsilon)+\frac{\partial}{\partial x_i}(\rho \varepsilon u_i)=\frac{\partial}{\partial x_j}\left[\left(\mu+\frac{\mu_t}{\sigma_\varepsilon}\right)\frac{\partial \varepsilon}{\partial x_j}\right]+C_{1\varepsilon}\frac{\varepsilon}{k}(G_k+C_{3\varepsilon}G_b)-C_{2\varepsilon}\rho\frac{\varepsilon^2}{k}+S_\varepsilon \quad [4]$$

In these equations, G_k represents the generation of turbulence kinetic energy, G_b is the generation of turbulence kinetic energy due to buoyancy and Y_M represents the contribution of the fluctuating dilatation in compressible turbulence to the overall dissipation rate. $C_{1\varepsilon}$, $C_{2\varepsilon}$ and $C_{3\varepsilon}$ are constants while σ_k and σ_ε are the turbulent Prandtl numbers for k and ε, respectively [28].

Regarding solar radiation, there are several models of energy transfer in the form of radiation, however, since the focus of this work is not any specific model, the solar load will be used in all models. The solar load can be used to calculate radiation effects from the sun's rays, allowing an engineer to determine the solar heating effect inside a building.

For this model we will also activate the solar ray tracing, as shown in figure 17. The solar load model's ray tracing algorithm can be used to predict the direct illumination energy source that results from incident solar radiation and includes the effects of direct solar illumination as well as diffuse solar radiation in the ANSYS Fluent model [28].

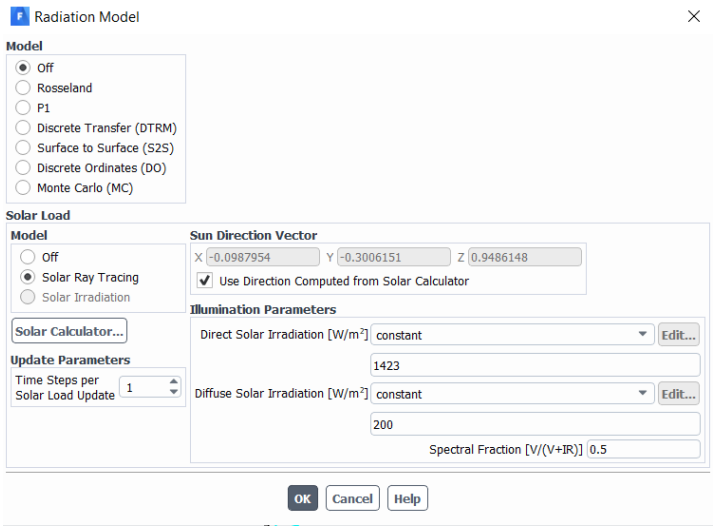

Figure 17: Radiation model with solar ray tracing on

The solar model associated with solar ray tracing also includes a solar calculator, useful for building the vector of the sun for a given time-of-day, date, and position. In this case, the coordinates of Porto were used, as shown in figure 18.

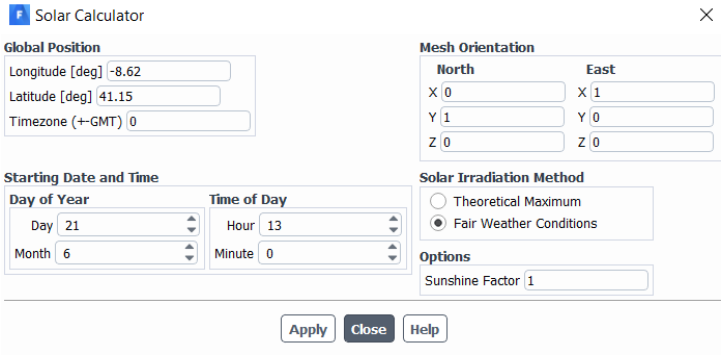

Figure 18: Solar calculator

The materials properties as well as the boundary conditions and the numerical procedure are described below.

3.2.1. AIR AND MATERIAL'S PROPERTIES

The properties of the solid materials required for the simulation are the density (ρ), thermal conductivity (k) and specific heat (Cp).

Once the models include a house, the materials involved in a wall, roof and floor are many. However, since the software does not accept the insertion of several materials, and consequently their densities, in the same element, it is necessary to calculate an equivalent density. The equivalent density was calculated from the individual density values of each material, obtained through ITE50 [29]. The materials used for the walls were bricks, mortar and polystyrene; for the roof were, concrete, mortar and polystyrene; and, lastly, the floor was made of concrete, mortar and polystyrene.

Regarding the photovoltaic panels and the box, the materials used were aluminum and polystyrene.

The thermal conductivity, λ, can be obtained using:

$$\lambda = \frac{e}{R} \quad [5]$$

where e is the thickness in meters, R is the resistance in m °C /W and the thermal conductivity units are W m-1 °C.

As for the specific heat, Cp, the vast majority of building materials have values between 800 and 1200 kg m-3, so a value in this range was chosen according to [30].

The density values of each element as well as their thermal conductivity and specific heat are shown in table 1.

Table 1:Materials Properties

Element	ρ (kg m^{-3})	λ (W m^{-1} °C)	Cp (J kg^{-1} °C^{-1})
Walls	1200	0.7	1000
Roof	1500	1	1000
Floor	1200	0.5	1000
PV Panels	2719	202.4	871
Box	25	0.04	850

The air was considered to be an ideal gas.

3.3. SIMULATION

MODEL 1: 1ST SIMULATION

In this first simulation, in all, the model used will be the k-epsilon and the radiation model will be the solar loading with solar ray tracing. The calculated solar vector corresponds to the first day of January at 10 am.

The boundary conditions considered for this simulation are shown in Table 2.

Table 2: Boundary conditions set in the first model

Boundary Type	Momentum	Thermal		
	Boundary Condition	Boundary Condition	T_0 / °C	Heat Transfer
Wall (Walls of the box)	No slip	Mixed	22	5
Wall (Roof of the house)	No slip	Mixed	22	1
Wall (PV Panel)	No slip	Mixed	22	5

Boundary Type	Radiation		
	Boundary Condition	Absorptivity	Transmissivity
Wall (Walls of the box)	Opaque	0.8	–
Wall (Roof of the house)	Opaque	0.8	–
Wall (PV Panel)	Opaque	0.8	–

All the walls were set with a non-slip condition, i.e., the fluid sticks to the wall and moves with the same velocity as the wall, if it is moving, which it is not in this case. The thermal boundary condition was considered mixed for all walls, meaning that heat transfer combines both radiation and convection. Data for the heat transfer coefficient were based on [31]. As for the free stream temperature, it was just assumed one: 22ºC in this case. In terms of radiation, all the elements were considered opaque, with the default options of fluent being maintained.

2nd Simulation

As in the previous simulation, the radiation and viscous models are the same. This simulation was run for January 1st at 10 am.

In this second simulation, the material of the box changes from aluminum to polystyrene, since aluminum due to is high thermal conductivity is not configured as the best option: it quickly absorbs heat as it emits. Besides the change of material, the geometry is also different: a box "outside" the box was made so that Fluent made a better distinction between the fluid and solid domain, with the original box representing the air.

The boundary conditions considered for this simulation are shown in Table 3.

Table 3: Boundary conditions set in the second simulation

Boundary Type	Momentum	Thermal		
	Boundary Condition	Boundary Condition	T_0 / °C	Heat Transfer
Wall (Walls of the box)	No slip	Mixed	20	5
Wall (Roof of the house)	No slip	Mixed	20	1
Wall (PV Panel)	No slip	Mixed	20	5

Boundary Type	Radiation		
	Boundary Condition	Absorptivity	Transmissivity
Wall (Walls of the box)	Opaque	0.8	–
Wall (Roof of the house)	Opaque	0.8	–
Wall (PV Panel)	Opaque	0.8	–

All the walls were set with a non-slip condition and the thermal boundary condition was, once again, considered mixed for all walls. The radiation conditions are the same as previously. The free stream temperature was changed to 20º in this simulation.

3rd Simulation

The viscous and radiation models are once again the same as previously used. The geometry was only changed for the second simulation, being the same as shown in figure 15 for this one.

In previous simulations, an issue related to solar heat flux was detected. Initially, the problem was wrongly attributed to the model geometry, but after several changes to it, the same result, in simulations made after it, was found. The cause was related to the properties of the photovoltaic panel, which had to be semi-transparent and not opaque, as until now.

The boundary conditions considered for this simulation are shown in Table 4.

Table 4: Boundary conditions set in the third simulation

Boundary Type	Momentum	Thermal		
	Boundary Condition	Boundary Condition	T_0 / °C	Heat Transfer
Wall (Walls of the box)	No slip	Convection	20	5
Wall (Roof of the house)	No slip	Radiation	20	1
Wall (PV Panel)	No slip	Convection	20	5

Boundary Type	Radiation		
	Boundary Condition	Absorptivity	Transmissivity
Wall (Walls of the box)	Opaque	0.8	–
Wall (Roof of the house)	Opaque	0.8	–
Wall (PV Panel)	Semi-transparent	0	1

All the walls were set with a non-slip condition. The heat transfer wall boundary chosen for the walls of the box and the PV panels was convective while the thermal boundary condition considered for the roof of the house was radiation. Data for the heat transfer coefficient were based on [31]. The free stream temperature considered it is the same as the previously simulation. As for the absorptivity and transmissivity, the ideal situation of total transmissivity was considered to test this condition, which makes the panel totally transparent in reality.

In addition to these simulations, another hypothesis, which consisted of calculating a heat generation rate, was tested and, although, the results were good, the simulation associated with the solar heat flux was more realistic, so this "theory" was discarded.

After these three simulations, six more will be made: three corresponding to a typical winter day and three others corresponding to a typical summer day. The highest temperature resulting of each one of these simulations will be considered the inlet temperature for the simulations of the second model. The highest temperature was chosen as a proof of concept, i.e., if the results obtained in the second model are not considered good, if the indoor temperature does not increase, with the highest temperatures being used, then it will not happen with lowest temperatures as well.

This parametric analysis was performed for January 1st and August 15th at 10 am, 1 pm and 4 pm, which means simulations 1 to 3 correspond to January 1st at 10 am, 1 pm and 4 pm respectively and simulations 4 to 6 to August 15th at the same hours.

These simulations have the same boundary conditions as the ones chosen for the third simulation. The only parameter chosen was temperature, as it was the only one that differed from the others. Table 5 represents a scheme of the cases chosen. The temperatures considered were taken from a climate file that was provided.

Table 5: Simulations made for the parametric analysis of inlet temperatures

Simulation	T_0 / °C
1	14.6
2	18.5
3	18.5
4	17.4
5	20.4
6	21.5

MODEL 2: 1ST SIMULATION

In this simulation, the viscous model used will once again be k-epsilon. As mentioned in 3.1.1, this model consists of a house with a circular air inlet and a window as an outlet, so no radiation model will be used, since what is being studied is the air flow. The objective is to analyze the contribution of heated air from the panels to the heating of the house, and therefore to the thermal comfort.

The inlet temperature considered in this simulation was 40ºC while the initial temperature of the house was set at 18ºC. The inlet temperature was 40ºC because for this first test a sufficiently high temperature was intended, since the greater the temperature difference, the greater the heat transfer. As for the initial temperature, it was 18ºC because that is the minimum comfort temperature in winter.

The boundary conditions considered for this simulation are shown in Table 6.

Table 6: Boundary conditions set in the second model

Boundary Type	Momentum			Thermal		
	Boundary Condition	v_0 / m s^{-1}	P_0 / Pa	Boundary Condition	T_0 / °C	Heat Transfer
Inlet	Velocity	1	–	Temperature	40	–
Outlet	Pressure	–	0	–	–	–
Wall (Walls of the house)	No slip	–	–	Convection	20	4
Wall (Roof of the house)	No slip	–	–	Convection	20	4
Wall (Floor of the house)	No slip	–	–	Convection	20	4

All the walls were set with a non-slip condition. The thermal boundary condition was considered convective for all walls. Data for velocity inlet was considered based on [32,33]. The free stream temperature was, like in the other simulations made, assumed.

A few more simulations were made in the follow-up of this, with small changes regarding the inlet temperature, the temperature of the house, among others, but nothing very significant. Therefore, with this first simulation having results considered positive, the simulation was considered "optimized" and served as a model for the next six simulations.

The following simulations follow the six previously performed in the second model. Having reached the temperatures in the box for each of the days: 1/1 and 15/8 at 10am, 1pm and 4pm, respectively, these were considered the inlet temperatures for the following simulations.

These simulations have the same boundary conditions as the one done previously. The parameters chosen were velocity at the inlet, inlet temperature and backflow temperature at the outlet. Table 7 represents a scheme of the cases chosen. The backflow temperatures considered were also taken from the climate file provided.

Table 7: Simulations made for the parametric analysis of the house temperatures

Simulation	**1**	**2**	**3**	**4**	**5**	**6**
Inlet temperature	23 **°C**	27,5 **°C**	22,8 **°C**	35 **°C**	39 **°C**	36 **°C**
Inlet velocity	v_1= 1 **m s^{-1}**	v_1= 1 **m s^{-1}**	v_1= 1 **m s^{-1}**	v_1= 1 **m s^{-1}**	v_1= 1 **m s^{-1}**	v_1= 1 **m s^{-1}**
Backflow temperature	14.6 **°C**	18.5 **°C**	18.5 **°C**	17.4 **°C**	20.4 **°C**	21.5 **°C**

In these simulations one of the parameters considered was the backflow temperature at the outlet, which did not happen in the first simulation of this model. The backflow temperature sets the total temperature of the inflow stream if the flow reverse direction.

After the data obtained in the simulations carried out in the two models considered, simulations in the macro model would be performed, as mentioned in 3.3.1, to see how, not only one, but six panels now would contribute to the thermal comfort of the house. However, for reasons of compliance with the deadline, this was not possible. These simulations are, thus, the future step of this study.

Still, conclusions about the relevance of performing them, or not, will be presented in chapter 5.

3.4. NUMERICAL PROCEDURE

Numerical simulations were performed using the commercial CFD package ANSYS® Fluent. The mesh was created using ANSYS® Meshing. The ideal mesh is the one that has the least computing time needed without compromising the results.

After using SpaceClaim to build all the geometries, the geometry files are imported to Meshing. In Meshing, the option CFD in physics preference was chosen and for the first model, the mesh was generated by selecting the option generate mesh, as shown in figure 19. Figure 20 shows the final mesh of the first model.

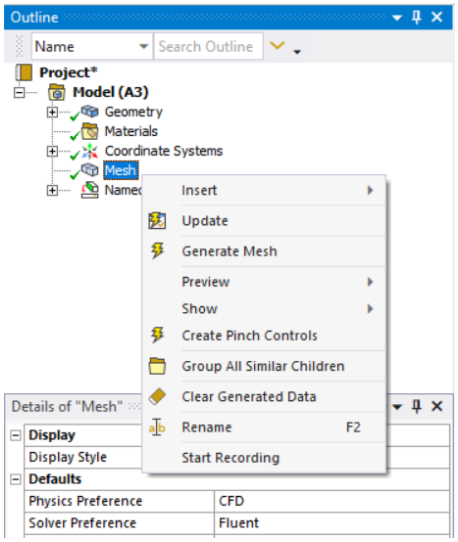

Figure 19: Generate mesh option

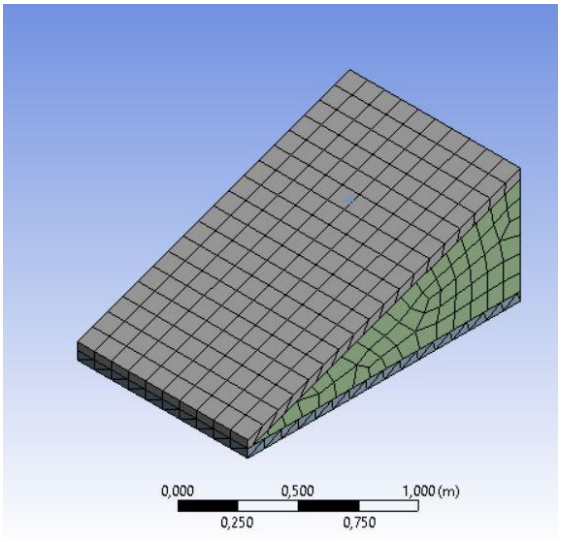

Figure 20: Final mesh of model 1

For the second model the mesh needed more refinement, since the window zone was less refined, i.e., the mesh had less elements, than the inlet zone with just the generate mesh option. Therefore, the option refinement in mesh was inserted and the level 3 of refinement was chosen. Figure 21 shows the comparison between the model with just the generate mesh option and with refinement.

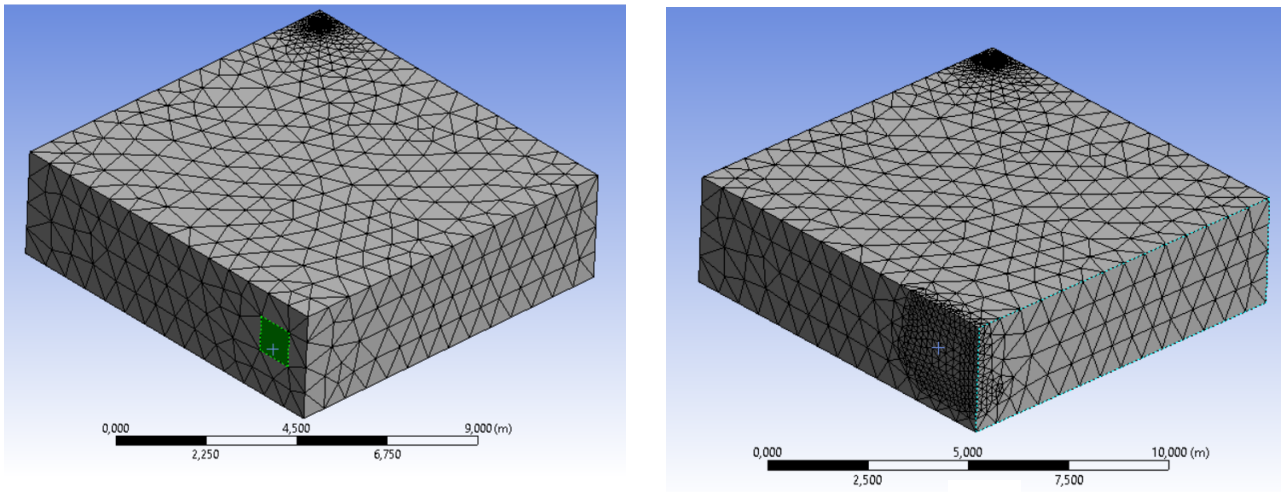

a) *b)*

Figure 21: Comparison of meshes in model 2; a) Mesh without refinement; b) Mesh with refinement

A number of mesh elements of 1760 and 23765 were used in the first and second model, respectively. Additionally, a grid independence test was done for the second model to understand if the results obtained were due to the mesh or to the backflow parameter, which will be explained in more detail in chapter 4. Table 8 shows the meshes used for the independence study.

Table 8: Meshes used for the mesh independence study

Mesh Number	Number of Elements
1	23765
2	132318

The conditions considered for this test correspond to the same used for the first of January in the parametric analyzes. Figure 22 shows the temperatures obtained in both cases:

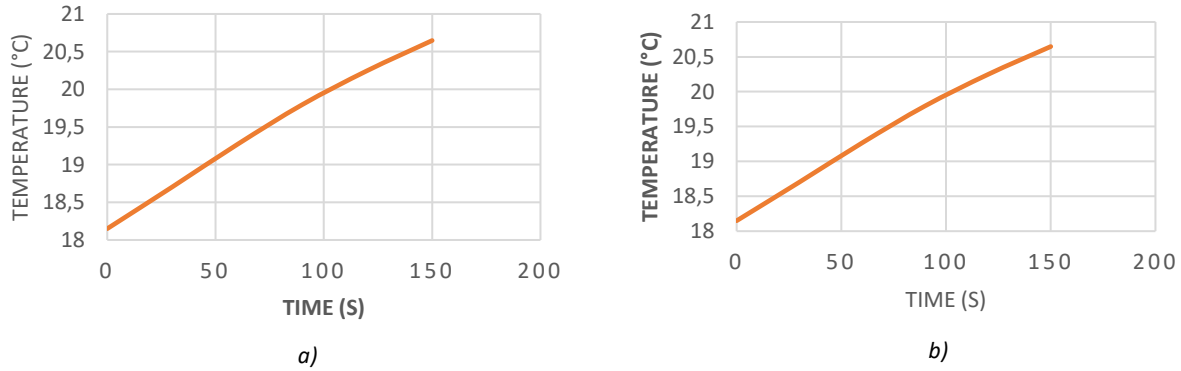

Figure 22: Temperatures obtained in both meshes; a) mesh number 1; b) mesh number 2

It is safe to consider that there is no significant difference between both meshes. Thus, it can be concluded that the mesh is not the problem of the results obtained.

Gravity was considered with value of -9.8 m/s^2 in the same direction of the axis of symmetry.

The momentum and energy equations were discretized by the Second Order Upwind scheme [29] and the pressure equation by the body force weighted [29]. The Standard Initialization was chosen [29]. The convergence criterion was that the scaled residuals were below 10^{-3} and 10^{-6} for the continuity equation and the energy equation, respectively.

Throughout this work some aspects, like the panels, were simplified. A photovoltaic panel is essentially made of silicon cells, a glass cover, and an aluminum frame, however for the simulations the material considered was only aluminum. The structure of the panel itself was simplified in geometry, in order to facilitate the simulations. In addition to the panel, the model of the house was also simplified, with no obstacles to the flow inside, which would involve more variables or "problems" with the software.

In terms of difficulties, the simulation time, initially, was a problem. In the beginning, the simulation time was supposed to be a year or a whole day with the temperature changing every hour, but after a few simulations it was clear that Fluent does not work very well with long periods of time, so it had to be adjusted to smaller intervals. Moreover, the Fluent software has a lot of details, so, deciding what radiation or viscous model was better, or what boundary conditions to choose, if the thermal boundary condition should be mixed or convection or other, for example, was difficult, since every option regarding the inputs could lead to a different result.

4
RESULTS AND DISCUSSION

4.1. INTRODUCTION

In this chapter, the results obtained from the simulations described in chapter 3 are presented and analyzed.

Thus, the temperatures distributions inside the panel and the house as well as the velocity magnitude distribution of the air inside the house will be obtained.

4.2. SIMULATIONS OF MODEL 1

4.2.1. FIRST SIMULATION

The results of the three simulations of the first model described in 3.3 are presented below. Figures 23 and 24 show the temperature distribution of the first simulation of model 1, whose time of simulation was thirty minutes. In this first simulation, the box and the panel start with a 20.2ºC temperature and heat up until 22ºC. Although the temperature increased almost two degrees, the free stream temperature was set at 22ºC, as shown in table 2, so, in normal conditions, it was expected that the temperature of both elements would surpass the exterior one.

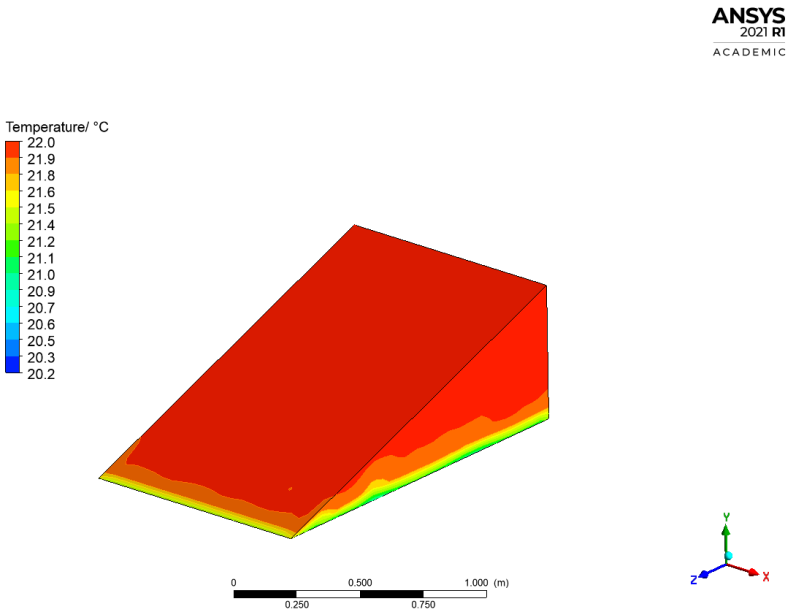

Figure 23: Temperature distribution of the first simulation

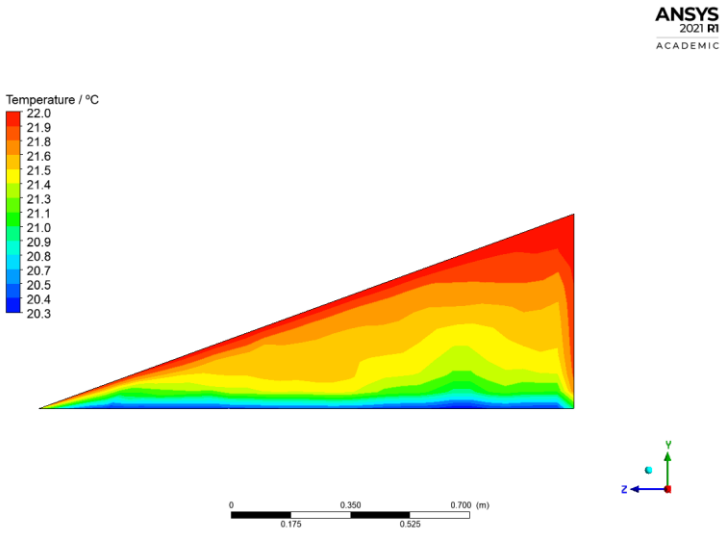

Figure 24: Plane view of the temperature distribution

Figure 25 shows the solar heat flux in this simulation. The fact that solar heat flux is null throughout the model explains why the temperature has not exceeded the previously defined, because even though there was an increase of temperature, it was not due to the solar power, but only to the outside temperature. Therefore, the maximum temperature would never be superior to the 22ºC initially defined.

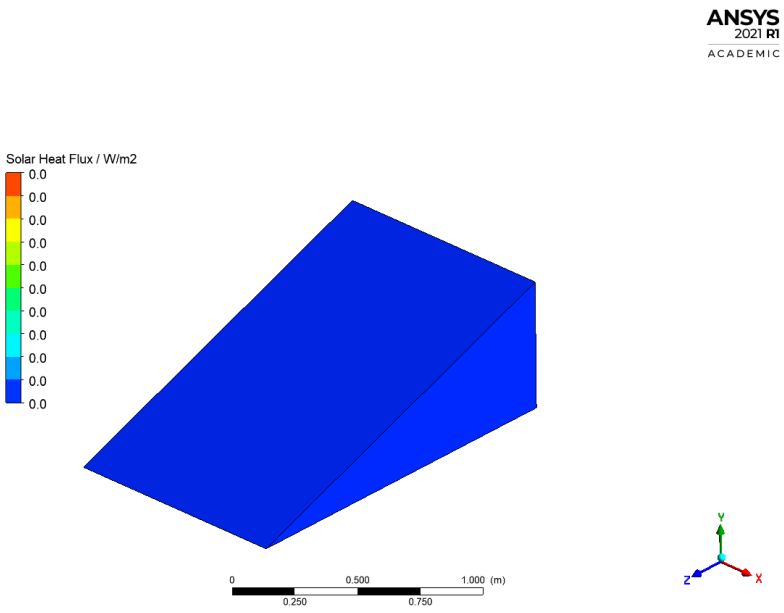

Figure 25: Solar heat flux of the first simulation

4.2.2. SECOND SIMULATION

Figures 26 shows the temperature distribution of the second simulation of model 1. In this second simulation, the initial temperature is 19ºC and the maximum temperature obtained is 120.5ºC. Through the figure it is possible to verify that, except for a small part, the entire model has a temperature of 19ºC, which is not plausible, and that the small part that has a heterogeneous distribution of temperatures heats up to 120.5ºC, which is unrealistic. Considering that the free stream temperature was set at 20ºC, and the simulation time was thirty minutes, this temperature value could never be reached.

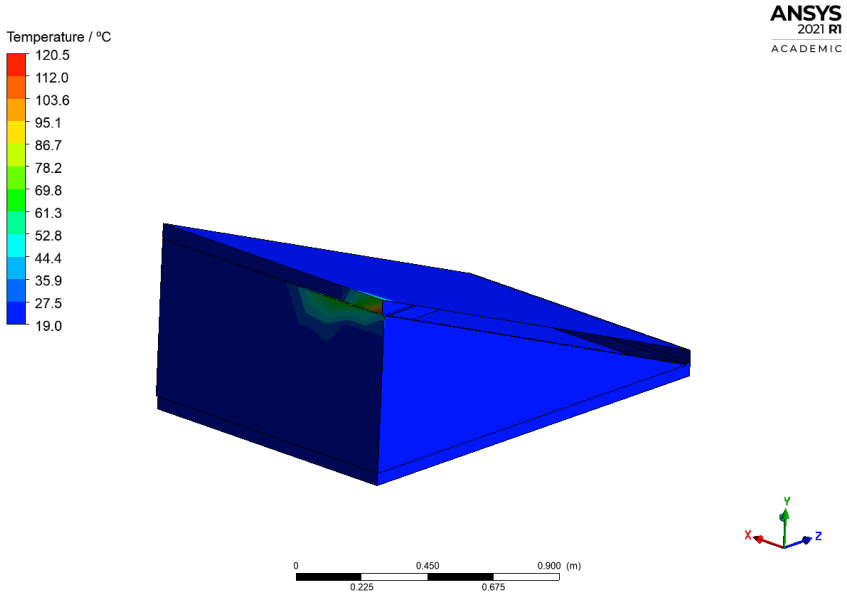

Figure 26: Temperature distribution of the second simulation

Figure 27 shows the solar heat flux in this simulation. The solar heat flux ranges between 0.8 W/m^2 and 1059.4 W/m^2, which is a big discrepancy of values, and it is possible to notice that the solar heat flux variation occurs in the same zone where the temperature increases drastically. Thus, the zone in which the variation occurs corresponds to the position of the solar vector.

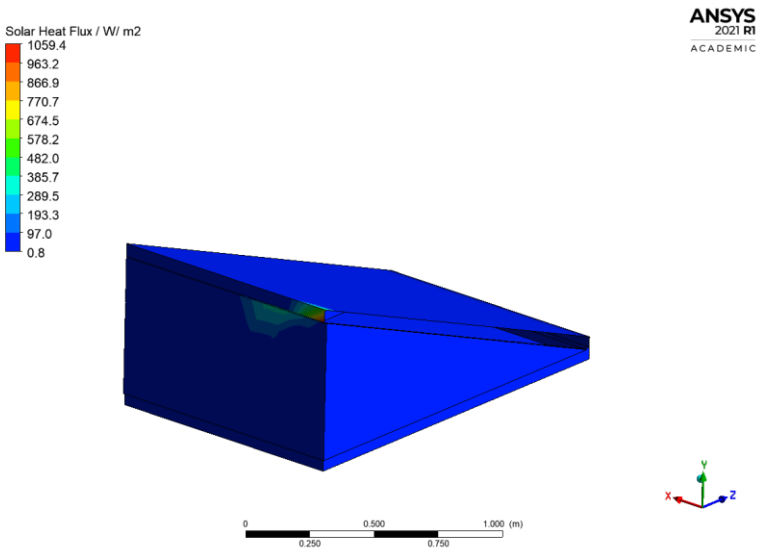

Figure 27: Temperature distribution of the first simulation

In this simulation, as mentioned in the previous chapter, the geometry was changed, and errors may result from that. Therefore, taking into account the results obtained, this simulation was not considered successful.

4.2.3. THIRD SIMULATION

Figures 28 and 29 show the temperature distribution in model 1 for the third simulation, that was the simulation considered successful. In this one, the initial temperature is 20.4ºC and the maximum temperature reached is 30.9ºC. The average temperature of the air inside the box is approximately 27ºC, as shown in figure 30.

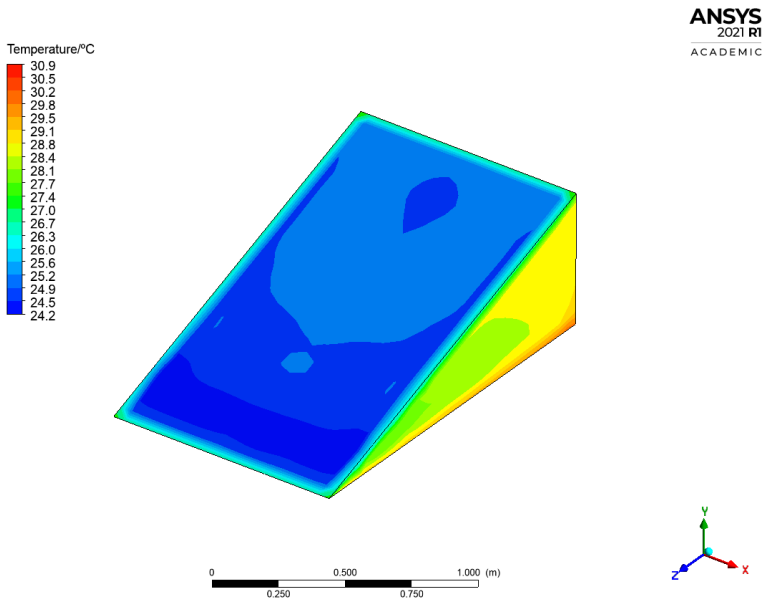

Figure 28: Temperature distribution of the third simulation

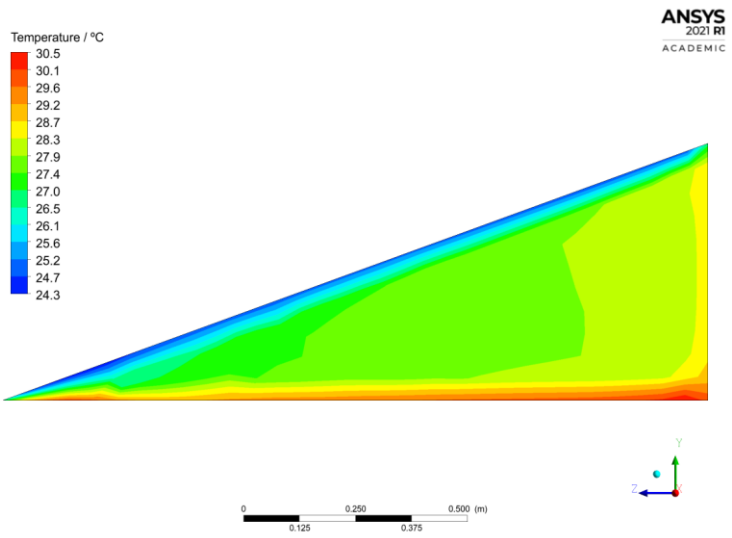

Figure 29: Plane view of the temperature distribution for the third simulation

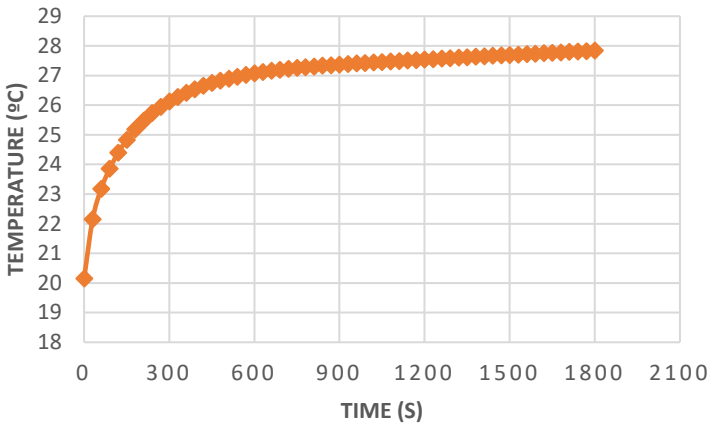

Figure 30: Average temperature inside the box

The results obtained in this case are, in comparison to the previous ones, much more plausible. This simulation, as well as the others, run for thirty minutes, and in this period an increase of approximately 7ºC was observed in both the air temperature inside the box and in the panel plus box set. The free stream temperature was set at 20ºC, again. Contrary to what happened in the previous simulations, in this one the different elements have different temperatures and the maximum temperature reached is higher than the outside temperature.

The fact that the panel has the lowest temperature is justified by its semi-transparent property, as mentioned in the previous chapter which, consequently, leads to a higher temperature in the box, something that Figure 28 also illustrates.

Figure 31 shows the uniform distribution of solar heat flux, whose value is 19.10 W/m^2. The temperature results already indicated that there was solar heat flux, and now it is possible to justify why those results were obtained. It is also important to highlight the difference between this heat flux value and the one obtained previously, with this one being undoubtedly much more realistic, especially since it is in winter.

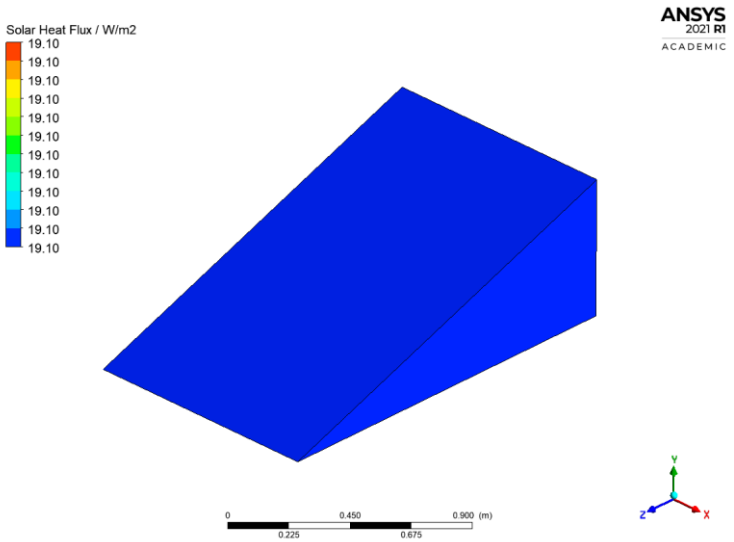

Figure 31: Solar heat flux for the third simulation

4.2.4. PARAMETRIC ANALYSIS

Since the results in the previous simulation were positive, i.e., they were credible, a parametric analysis was performed as mentioned in 3.3. on January 1st and August 15th at 10 am, 1pm and 4 pm.

This analysis aims to understand what temperatures are obtained for the different hours of the same day, in a summer and winter season. These temperatures will then be used in further simulations so that a conclusion can be draw as to the feasibility of the solution under study. Figures 32 and 33 show the average temperatures reached inside the box for the two days considered and figures 34 and 35 show the comparison of the temperatures obtained on both days.

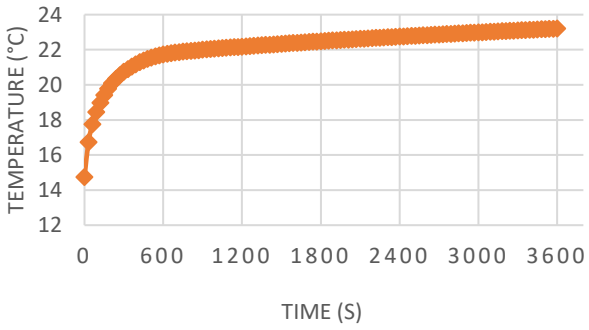

a)

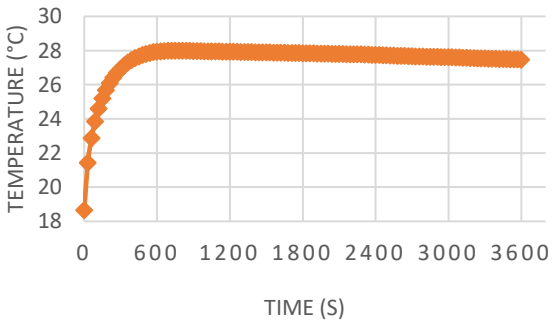

b)

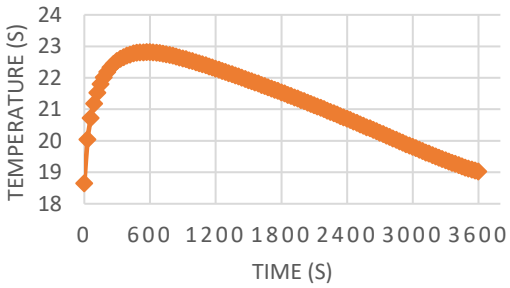

c)

Figure 32: Average temperature in the box for 1/1: a) simulation at 10 am; b) simulation at 1 pm; c) simulation at 4 pm

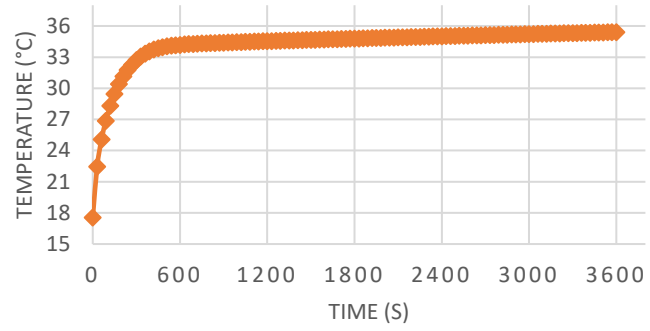

a)

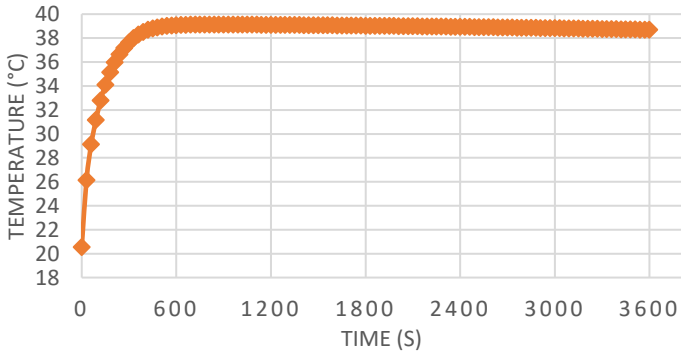

b)

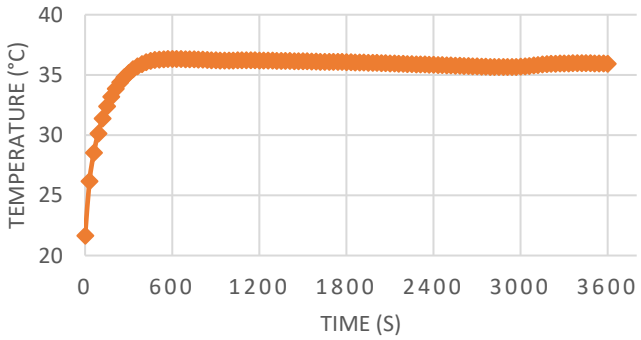

c)

Figure 33: Average temperature in the box for 15/8: a) simulation at 10 am; b) simulation at 1 pm; c) simulation at 4 pm

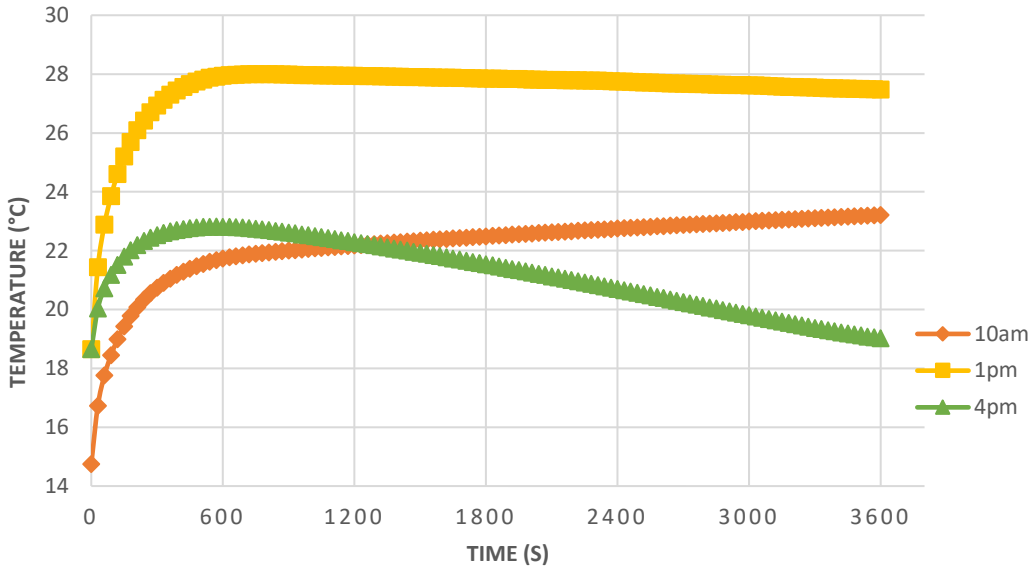

Figure 34: Temperature comparison for January 1st

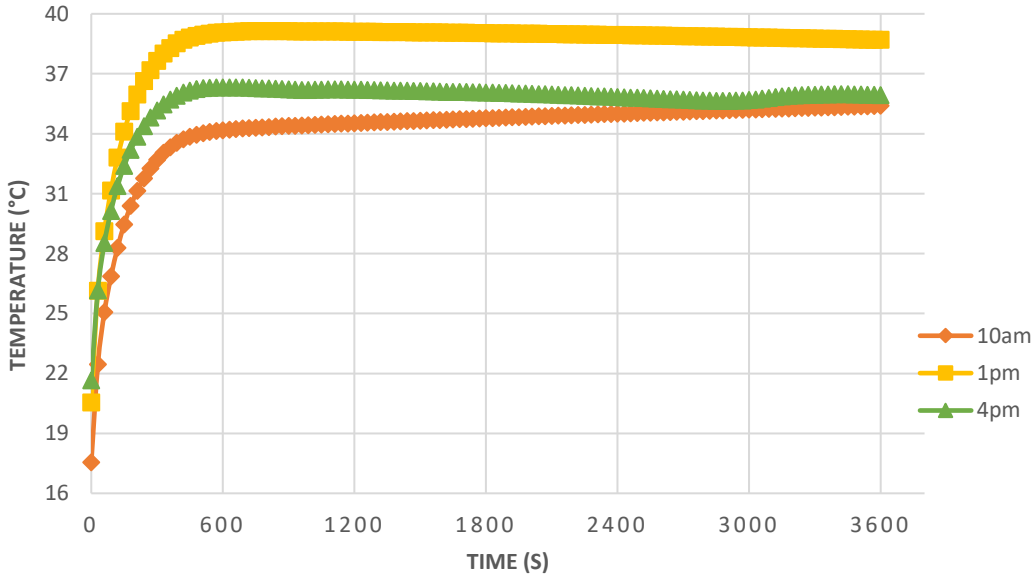

Figure 35: Temperature comparison for August 15th

As it would be expected, comparing the two days under study, the temperatures obtained in summer are much higher than in winter. The maximum temperature reached in winter is approximately 27.5ºC at 1 pm while the minimum is 19ºC at 4 pm. As far as summer is concerned, the maximum temperature is 39ºC, also at 1 pm, and the minimum is around 34ºC at 10 am. Although these results were expected, the ideal for the solution in question was that the reverse would happen, i.e., the solution under study aims to recover the heat produced from the photovoltaic panel and use it to heat a house. Since it is in

winter that temperatures are lower and this heating is more needed, the ideal would be to have temperatures obtained in summer, in winter.

Contrary to what happens in the other graphs, it is possible to see that the temperature at 4 pm on January 1st (figure 32c)), after its peak, progressively decreases. This happens because it is winter and the solar heat flux is lower at this hour, in comparison to the other two. However, once this result was a little different from the obtained at 10 am and 1 pm, a simulation starting at 10 am until 8 pm was carried out, to "prove" that the solar heat flux is, indeed, lower, as shown in Figure 36.

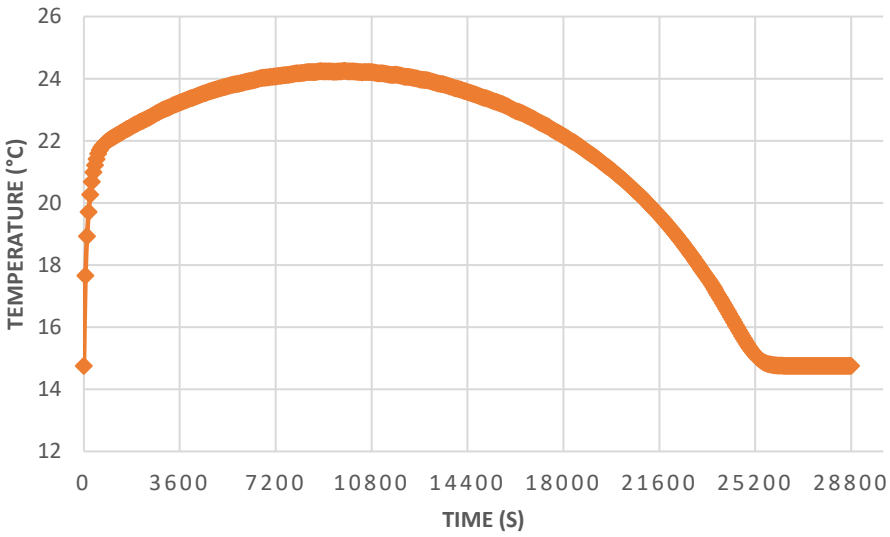

Figure 36: 8 hours simulation in winter

With this graph it is possible to verify that from 3 pm onwards, the temperature begins to decrease, which corroborates the information provided by Figure 32c), in which after just 10 minutes, the temperature begins to drop. In addition to this graph, Figures 37 and 38 show the solar heat flux at 4 pm and at the end of the eight hours of simulation, noting that at 4 pm the flow is very low and at the end of the eight hours is non-existent (at 8 pm we will not have any radiation), which explains, once again, the temperature decrease. Since it is a winter day, this is normal, as the number of hours of sunshine are lower.

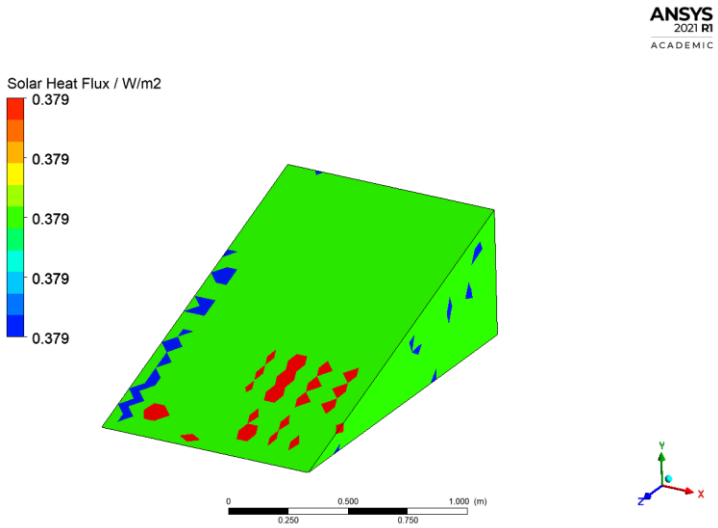

Figure 37: Solar heat flux at 4 pm on January 1st

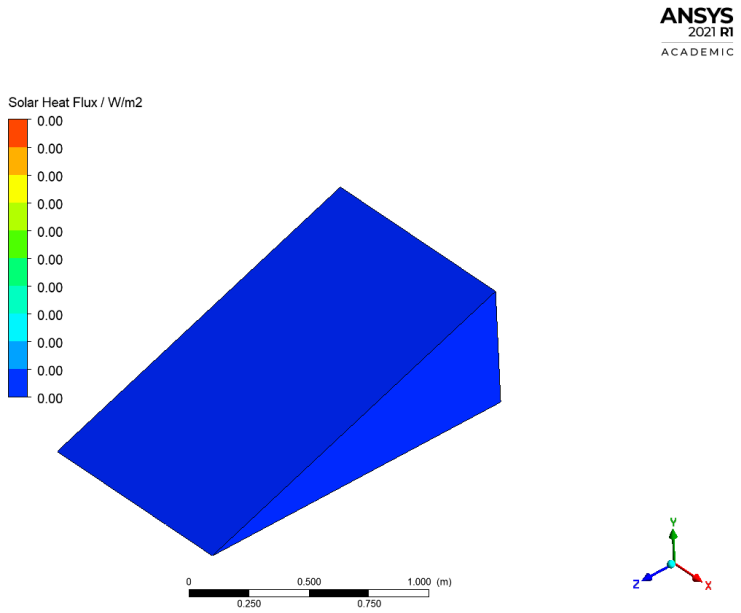

Figure 38: Solar heat flux at the end of the 8 hours simulation

Figure 39 shows the contrast between solar radiation in winter and summer. In summer, after eight hours of simulation there is no sharp drop in temperature, which is normal, since there are more hours of sunshine, and consequently greater solar radiation. Once the main focus of this work is the temperatures obtained for winter, the only objective of this graphic is to show the temperature difference between winter and summer.

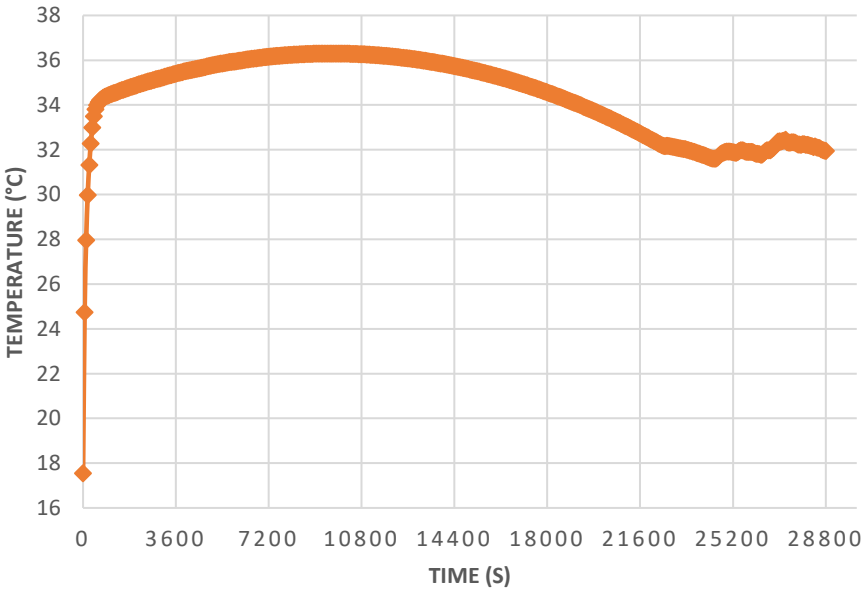

Figure 39: 8 hours simulation for August 15th

4.3. SIMULATIONS OF MODEL 2

Figure 40 shows the average temperatures obtained in the house with a circular duct inlet and a window as an outlet, when the free stream temperature is set at 20ºC and the inlet temperature at 40ºC. The maximum temperature reached is 25º, where it then stays stable. The temperature stays at 25ºC because, even though, the air entering the house is at a high temperature, the air coming from the window is much lower, which prevents the house of heating more.

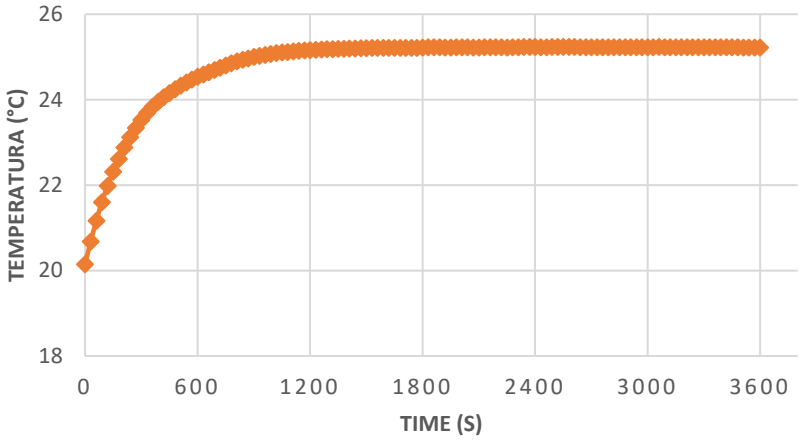

Figure 40: Average temperature inside the house

As mentioned previously, considering the inlet temperature, 25°C as the maximum temperature may seem low, however, this happens because there is reverse flow, as illustrated in figures 41,42 and 43. Reverse flow means that the flow wants to re-enter the domain at the location where the outlet is placed, so, in this case mean that the air is re-entering in the house through the window.

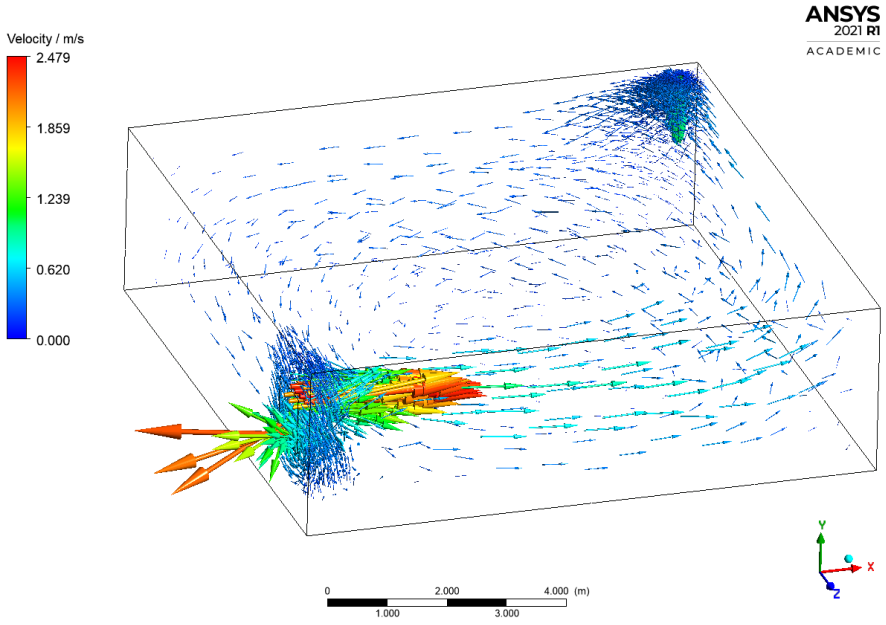

Figure 41: Velocity magnitude distribution of the air inside the house

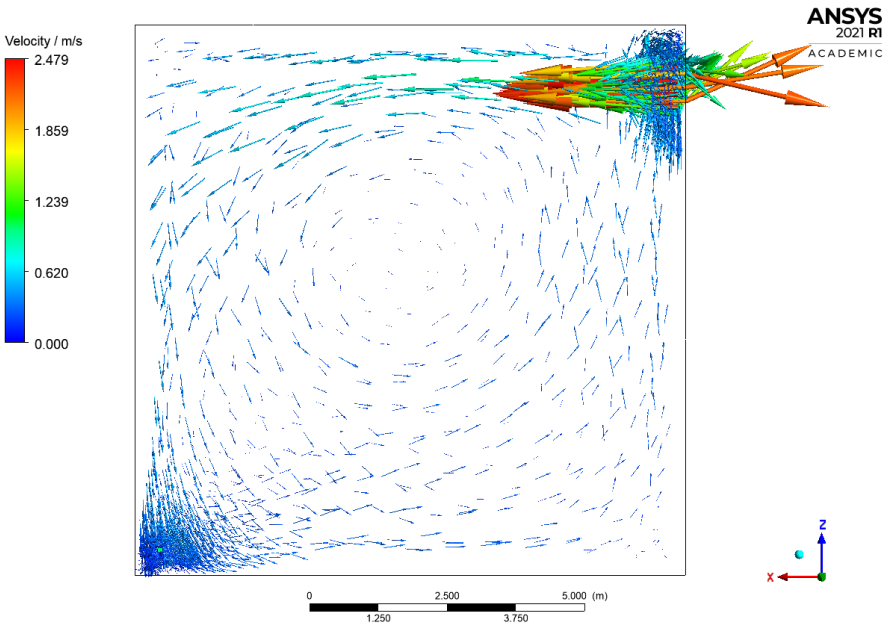

Figure 42: Top view of figure 35

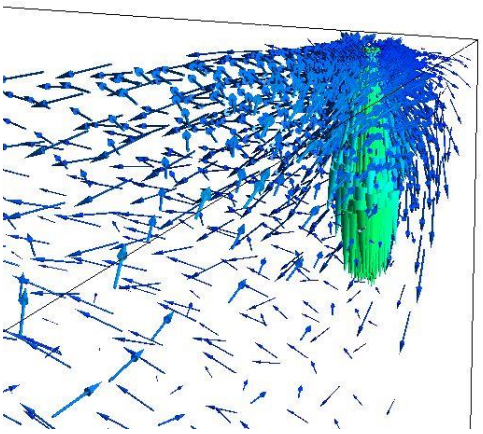

Figure 43: Zoom in of the inlet

Figure 41 shows the velocity magnitude distribution inside the house. The air enters the house with a velocity of 1 m/s and exits with velocities between 1.25 and 1.86 m/s. These figures allow to understand how the air circulates inside the house and, in addition to losses due to natural convection, it is possible to verify that there is also a large air inlet through the window.

The temperature at which this air enters as well as the velocity at which it enters, that is in this case higher than the inlet one, when compared, are crucial for the heating or cooling of the house and can explain the results obtained.

Although the backflow temperature, i.e., the total temperature of the inflow stream if the flow reverse direction, was not taken into consideration when doing this simulation, this image allows to understand the importance of it. Since, at the time, this parameter was not considered, its temperatures was by default set at 26.85ºC, which explains why with 40ºC, the temperature reached was only of 25ºC.

4.3.1. PARAMETRIC ANALYSIS

As for the first model, a parametric analysis was performed for this one on January 1st and August 15th at 10 am, 1 pm and 4 pm.

If the first analysis had the objective of finding out what temperatures were obtained inside the box, this one intends to determine the temperature inside the house. For these simulations, the inlet temperatures determined in the previous parametric analysis were used. The values are shown in table 7.

Figures 44 and 45 show the average temperatures reached inside the house for the two days considered.

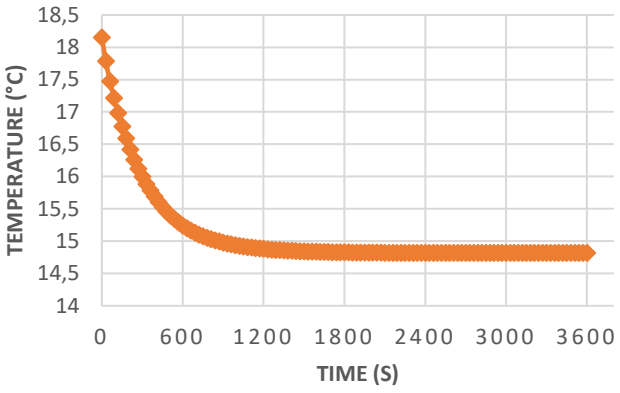

a)

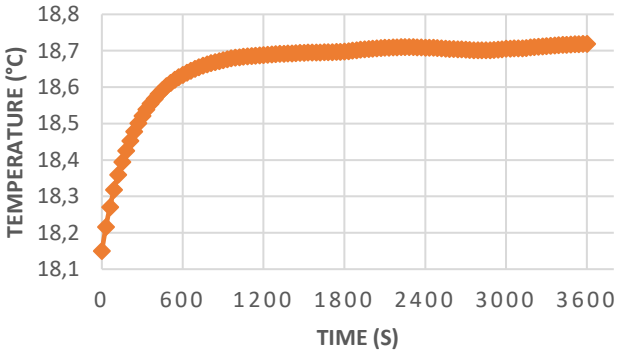

b)

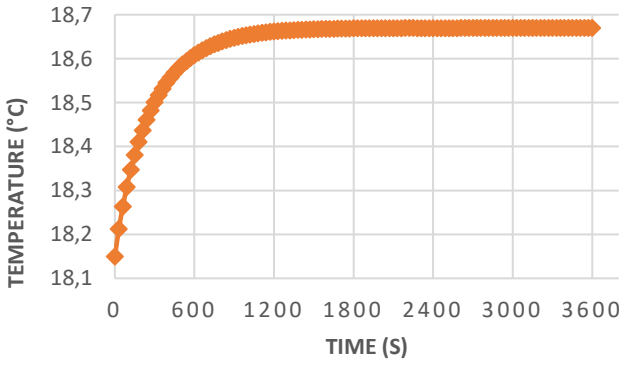

c)

Figure 44: Average temperature in the house for 1/1: a) simulation at 10 am; b) simulation at 1 pm; c) simulation at 4 pm

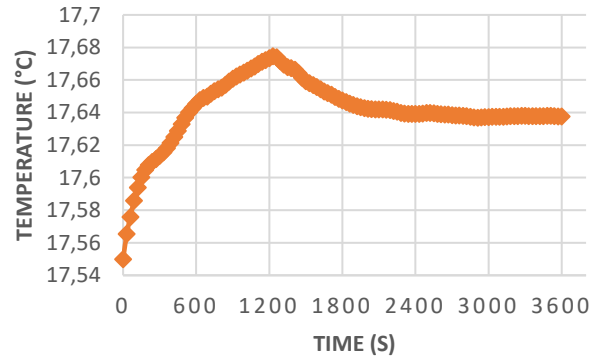

a)

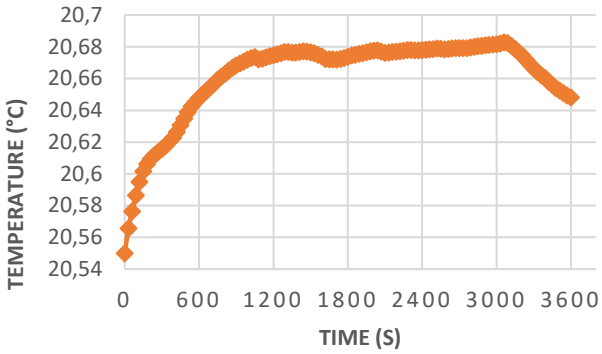

b)

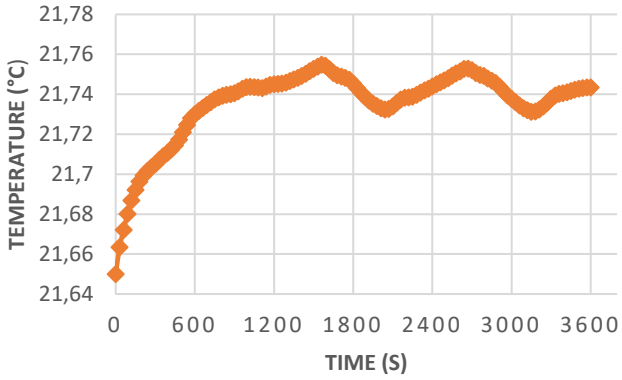

c)

Figure 45: Average temperature in the house for 15/8: a) simulation at 10 am; b) simulation at 1 pm; c) simulation at 4 pm

Similar to what happened in the box simulations, temperatures are, in general, higher inside the house in summer.

For the 1st of January, all simulations started from the minimum comfort temperature, i.e., 18ºC, and it is possible to observe that in Winter the temperature inside the house tends to equal the outside temperature. This can be explained, as previously, by the existence of reverse flow, as shown in figures

46 and 47. Once again, like in the previous parametric analysis, summer is only being considered so that a comparison with winter can be established.

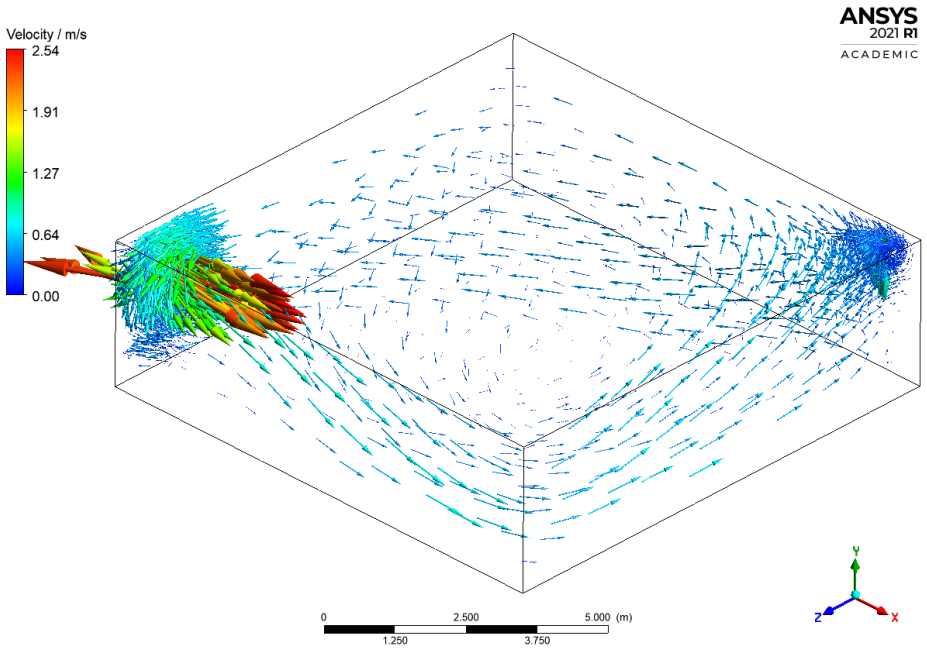

Figure 46: Velocity magnitude distribution of the air inside the house on 1/1 at 1 pm

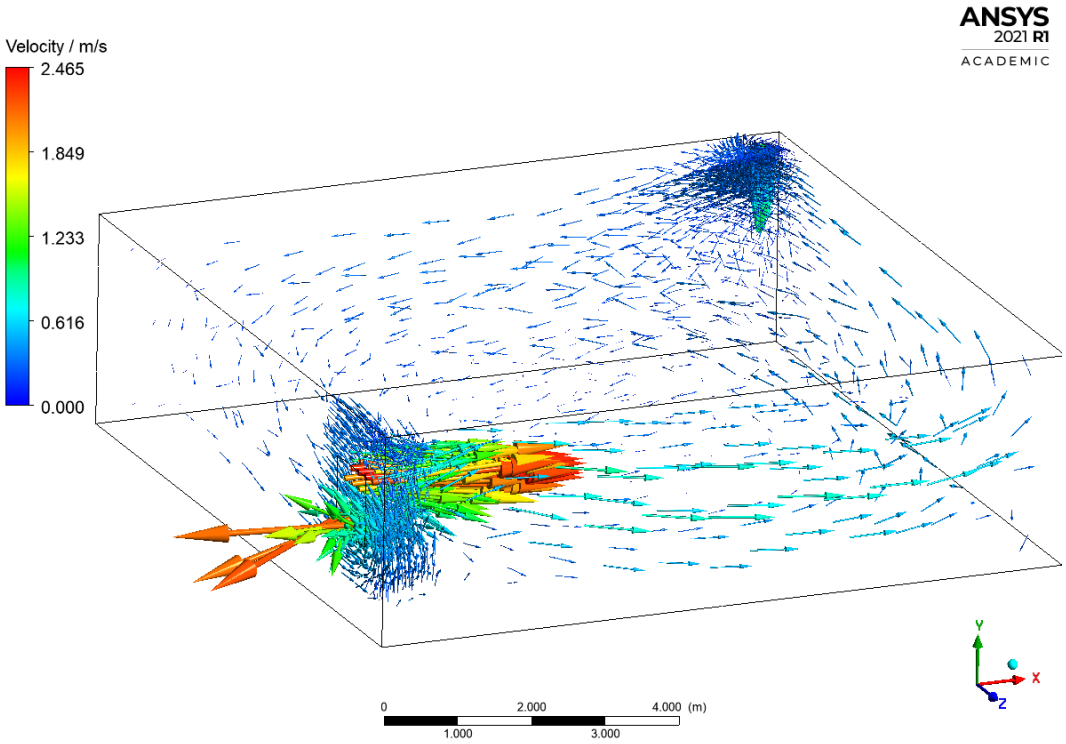

Figure 47: Velocity magnitude distribution of the air inside the house on 15/8 at 1 pm

One of the parameters taken into account in these simulations, since it was perceived in the previous one that it was fundamental, was the backflow temperature, given the impact it had in the average temperature reached inside the house. The backflow temperature values are shown in table 7.

This parameter justifies the results obtained, since in winter, as temperatures are lower, the inlet temperature is not sufficient to heat the house. Regarding summer, although there is an increase in temperature, it is not significant due to the disparity of values between the inlet and backflow temperatures. The velocity at which the air enter through the window, also explains these results and how fast the temperatures drop. The inlet velocity is 1 m/s for both days, with the exit velocity being between 1.257 m/s and 2.54 m/s on January 1st and between 1.23 m/s and 2.465 m/s on August 15th.

4.3.2. SIMULATION OF A HOUSE WITHOUT WINDOW

After realizing how the house would heat up with a window, an extra simulation without the window was made, to see if it would heat up this way. The simulation was run for the first day of January at 10 am. The boundary conditions considered were the same as the parametric analysis for the house with a window and the starting temperature was, once again, 18ºC.

Figure 48 shows the average temperatures obtained.

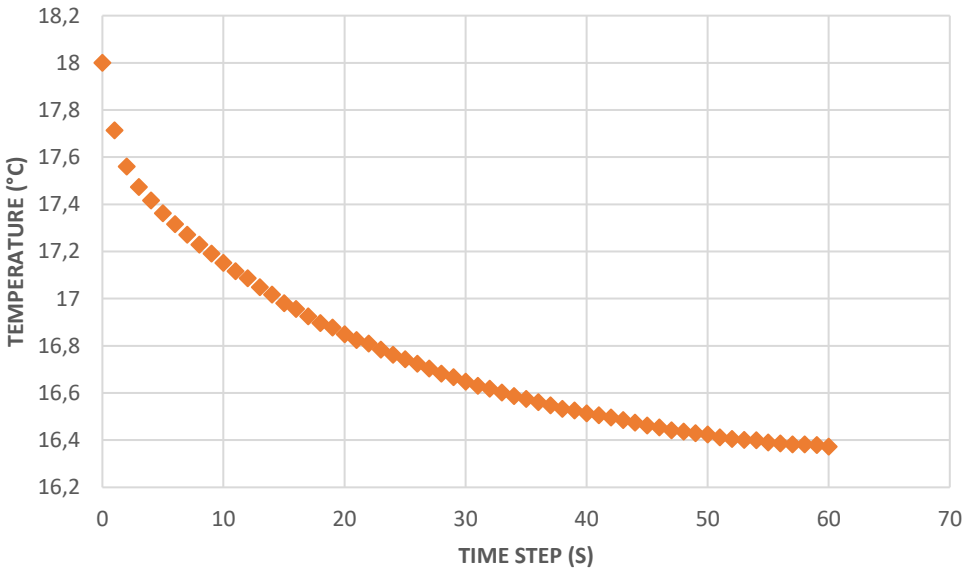

Figure 48: Average temperatures inside the house

Through the figure, it is possible to verify that, as in the previous simulations, the temperature also drops, which, at first, would not be expected.

Although we do not have a window, natural convection losses are greater than the heating provided by the system. If the walls of the house are considered as adiabatic, which means that there is no heat transfer between the walls, for the same conditions, there would be an increase of temperature, as shown in figure 49, which proves the reliability of the simulation made previously. If the inlet temperature was higher, then, the results obtained would, probably, also be different.

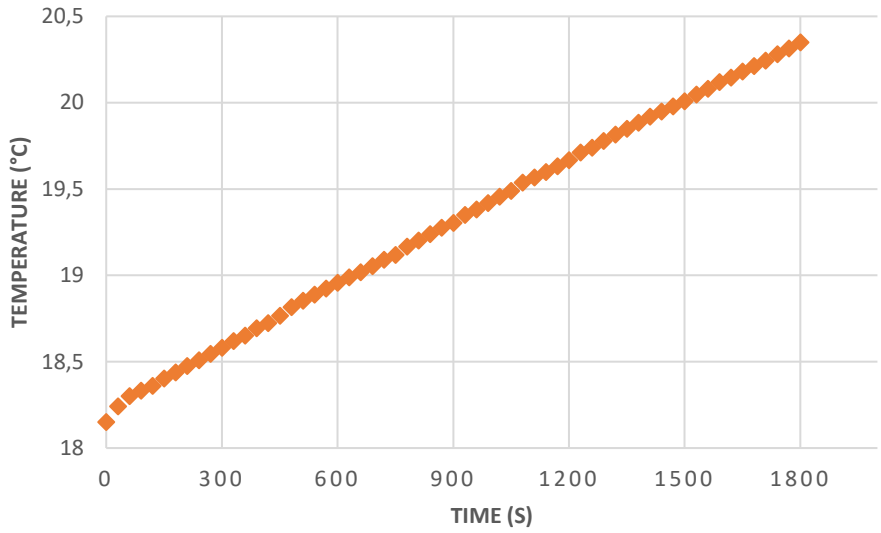

Figure 49: Average temperatures inside the house with adiabatic walls

5
CONCLUSIONS

5.1 GENERAL CONCLUSIONS

In this work, the feasibility of a photovoltaic panel solution installed on the roof was studied with the objective of recovering the heat that the panel would, indirectly produce as a consequence of its operation, and with use it to heat the indoor air, using numerical simulations for this purpose.

For this analysis, two models were used: one corresponding only to the panel with the box, that will store the heat, and other corresponding to the house with a duct, for the air inlet coming from the panel, and a window as an outlet. Through the simulations, the temperature profiles were obtained in both models, with the maximum temperature reached within the box being 30.9ºC and inside the house of approximately 25ºC.

Since the results obtained in the first simulations were plausible given the inputs considered, a parametric analysis was performed for a typical summer and winter day for both models. It should be noted that summer is not the focus of this work and was considered essentially so that a comparison with winter could be established (That is the season in which houses really need to be heated).

The results obtained for the first model show that the air inside the box did not heat up enough, that is, the temperatures obtained inside the box, in winter, are not high enough, something easily justified by the low amount of solar radiation in winter. When comparing winter temperatures with summer temperatures, the contrast is notorious. It is also important to point out that the heat flux is not constant, so these temperatures, already low, that will be used for the following simulations would not be constant all the time in reality, they would probably be even lower.

Following these simulations, the resulting maximum temperatures were used as the inlet temperatures for the parametric analysis in the house. The results obtained show that the house does not heat up, with the indoor temperature tending to equal the outdoor temperature. A subsequent simulation of the house without a window, and therefore without any type of ventilation, was made and it was concluded that the fact that the house does not heat is not due to the window, but rather to the fact that the heat provided by the panel is not high enough.

The next step of this work, which could not be carried out due to time constraints, consisted in the analysis of the simultaneous contribution of the six panels to the thermal comfort of the house, as initially proposed. However, and even though it was not possible to make those simulations, taking into account the results obtained, even if there were six panels, the volume of each one is only 0.5 m3, so even using all of them, based on the temperatures obtained previously, it would not be enough for the house to heat.

It can be concluded that, although the results obtained are interesting and the Ansys Fluent allows access to graphs, they too, very interesting, the solution under study is not feasible in winter, since solar radiation is not enough for heating using this contribution. However, this solution, although not avoiding the use of other heating means, can help in heating, contributing to the reduction of some needs.

5.2 FUTURE WORK

For future work it is suggested, as mentioned previously, that a simulation with all the panels would be performed, so that the conclusions could be more accurate, the results more substantiated, and the study more detailed, in general.

In a future approach it would also be interesting to add complexity to the geometry of the house and study optimal points for the hot air inlet. The model used in this work was very simplified, and it was showed by the results obtained that the heat coming from the back of panels was not enough to heat the house, but if the house had rooms and doors, for example, and the air inlet in "optimal" zones, it would be possible to heat a room instead of the whole house, which would also be useful.

Moreover, and taking this work as a starting point, other alternatives for recovering thermal energy can be studied, using the same simulation strategy for predicting results, since although it is not so widely used, Ansys Fluent has immense potential in the field.

REFERENCES

[1] IRENA (2019), Global energy transformation: A roadmap to 2050 (2019 edition), International Renewable Energy Agency, Abu Dhabi.

[2] IEA (2020), World Energy Outlook 2020, IEA, Paris https://www.iea.org/reports/world-energy-outlook-2020.

[3] APREN (2020), Anuário da Apren 2020.

[4] IRENA (2019), Future of Solar Photovoltaic: Deployment, investment, technology, grid integration and socio-economic aspects (A Global Energy Transformation: paper), International Renewable Energy Agency, Abu Dhabi.

[5] Portuguese Government. "Roadmap for Carbon Neutrality 2050 (RNC 2050)". Portugal, June 2019.

[6] National Geographic, "The evolution of solar technology", 2012 [Online]. Available: https://blog.nationalgeographic.org/2012/05/30/the-evolution-of-solar-technology/

[7] Clearway Community Solar, "The Evolution of Solar Panels", 2018 [Online]. Available: https://www.clearwaycommunitysolar.com/blog/understanding-community-solar/evolution-solar-panels/

[8] Vallêra, A., Brito, M.; "Meio Século De História Fotovoltaica." Gazeta de Física, 2006: 10-15.

[9] Tiantian Zhang, Meng Wang and Hongxing Yang. (2018) "A Review of the Energy Performance and Life-Cycle Assessment of Building-Integrated Photovoltaic (BIPV) Systems.

[10] Kumar, Nallapaneni Manoj, K. Sudhakar, and M. Samykano. (2019) "Performance comparison of BAPV and BIPV systems with c-Si, CIS and CdTe photovoltaic technologies under tropical weather conditions." Case Studies in Thermal Engineering 13: 100374.

[11] Lujean Ahmad, Navid Khordehgah, Jurgita Malinauskaite, Hussam Jouhara. (2020) "Recent advances and applications of solar photovoltaics and thermal technologies" Energy 207 (2020) 118254.

[12] Priscila Gonçalves Vasconcelos Sampaio, Mario Orestes Aguirre González. (2017) "Photovoltaic solar energy: Conceptual framework" Renewable and Sustainable Energy Reviews 74 (2017) 590–601.

[13] Deepak Paramashivan Kaundinya, P. Balachandra, N.H. Ravindranath. (2009) "Grid-connected versus stand-alone energy systems for decentralized power-A review of literature" Renewable and Sustainable Energy Reviews 13 (2009) 2041–2050.

[14] M.M. Fouada, Lamia A. Shihatab, ElSayed I. Morgana. (2017) "An integrated review of factors influencing the performance of photovoltaic Panels" Renewable and Sustainable Energy Reviews 80 (2017) 1499–1511.

[15] Mary Debbarma, K. Sudhakar, Prashant Baredar. (2016) "Comparison of BIPV and BIPVT: A review" Resource-Efficient Technologies 3 (2017) 263–271.

[16] National Renewable Energy Laboratory (NREL). Best Research-Cell Efficiencies. Available online: https://www.nrel.gov/pv/assets/images/efficiency-chart.png

[17] Subramanian Senthilkannan Muthu. (2020) "6 - Estimating the overall environmental impact of textile processing: Life cycle assessment of textile products" The Textile Institute Book Series.

[18] V.M. Fthenakis, H.C. Kim. (2011) "Photovoltaics: Life-cycle analyses" Solar Energy, Volume 85, Issue 8

[19] L.Lu, H.X.Yang. (2010) "Environmental payback time analysis of a roof-mounted building-integrated photovoltaic (BIPV) system in Hong Kong" Applied Energy Volume 87, Issue 12.

[20] Yinyin Fu, Xin Liu, Zengwei Yuan. (2014) "Life-cycle assessment of multi-crystalline photovoltaic (PV) systems in China" Journal of Cleaner Production 86 (2015) 180-190.

[21] Jinqing Peng, Lin Lu, Hongxing Yang. (2012) "Review on life cycle assessment of energy payback and greenhouse gas emission of solar photovoltaic systems" Renewable and Sustainable Energy Reviews 19 (2013) 255–274.

[22] Sakhr M. Sultan, M.N. Ervina Efzan. (2018) "Review on recent Photovoltaic/Thermal (PV/T) technology advances and applications" Solar Energy 173 (2018) 939–954.

[23] S.A. Kalogirou, Y. Tripanagnostopoulos. (2006) "Hybrid PV/T solar systems for domestic hot

water and electricity production" Energy Conversion and Management 47 (2006) 3368–3382.

[24] Tingting Yang n, Andreas K. Athienitis. (2016) "A review of research and developments of building-integrated photovoltaic/thermal (BIPV/T) systems" Renewable and Sustainable Energy Reviews 66 (2016) 886–912.

[25] Soteris A. Kalogirou. (2004) "Solar thermal collectors and applications" Progress in Energy and Combustion Science 30 (2004) 231–295.

[26] Bjørn Petter Jelle. (2012) "Accelerated climate ageing of building materials, components and structures in the laboratory" Journal of Materials Science volume 47, pages6475–6496.

[27] Henrik Davidsson, Bengt Perers, Björn Karlsson. (2009) "Performance of a multifunctional PV/T hybrid solar window" Solar Energy 84 (2010) 365–372.

[28] ANSYS, ANSYS Fluent Theory Guide, vol. 15317, no. November. 2013.

[29] Carlos A. Pina dos Santos, Luis Matias. *ITE 50 - Coeficientes de Transmissão Térmica de Elementos da Envolvente dos Edifícios*, LNEC, Lisboa, 2006.

[30] Vasco Peixoto de Freitas, Maria Isabel Torres, Ana Sofia Guimarães. *Humidade Ascencional*. FEUP, 2008.

[31] Y. A. Çengel, Heat and Mass Transfer - A practical approach, Third edit. McGraw-Hill Science/Engineering/Math, 2007.

[32] Rahul Khatria, Abhay Pratap Singha, Vaibhav Rai Khareb. (2016) "Identification of Ideal Air Temperature Distribution using different location for Air Conditioner in a room integrated with EATHE – A CFD based approach" Energy Procedia 109 (2017) 11 – 17.

[33] Ahmed A. Youssef, Ehab M. Mina, Ahmed R. ElBaz, Raouf N. AbdelMessih. (2017) "Studying comfort in a room with cold air system using computational fluid dynamics" Ain Shams Engineering Journal 1753-1762.